







# The dentary of hadrosauroid dinosaurs: evolution through heterochrony

by D. FREDRIK K. SÖDERBLOM<sup>1,\*</sup> , ALEJANDRO BLANCO<sup>2,4</sup> ,  
ALBERT PRIETO-MÁRQUEZ<sup>3</sup>  and NICOLÁS E. CAMPIONE<sup>1,5,\*</sup> 

<sup>1</sup>Palaeobiology Programme, Department of Earth Sciences, Uppsala University, Villavägen 16, 752 36 Uppsala, Sweden; [soderblom.fredrik@gmail.com](mailto:soderblom.fredrik@gmail.com), [ncampion@une.edu.au](mailto:ncampion@une.edu.au)

<sup>2</sup>SNSB-Bayerische Staatssammlung für Paläontologie und Geologie, Richard-Wagner-Straße 10, 80333 München, Germany; [alejandro.blancoc@udc.es](mailto:alejandro.blancoc@udc.es)

<sup>3</sup>Institut Català de Paleontologia Miquel Crusafont (ICP-CERCA), Universitat Autònoma de Barcelona, c/ Escola Industrial 23, 08201 Barcelona, Sabadell, Spain; [albert.prieto@icp.cat](mailto:albert.prieto@icp.cat)

<sup>4</sup>Current address: Facultade de Ciencias, Universidade da Coruña, Rúa da Fraga 10, 15008 A Coruña, Galicia, Spain

<sup>5</sup>Current address: Palaeoscience Research Centre, School of Environmental and Rural Science, University of New England, Armidale, NSW 2351, Australia

\*Corresponding author

Typescript received 19 December 2022; accepted in revised form 5 July 2023

**Abstract:** The near-global distribution of hadrosaurid dinosaurs during the Cretaceous has been attributed to mastication, a behaviour commonly recognized as a mammalian adaptation. Its occurrence in a non-mammalian lineage should be accompanied by the evolution of several morphological modifications associated with food acquisition and processing. This study investigated morphological variation in the dentary, a major element of the hadrosauroid lower jaw. Eighty-four hadrosauroid dentaries were subjected to geometric morphometric and statistical analyses to investigate their taxonomic, ontogenetic, and individual variation. Results suggest increased food acquisition and processing efficiency in saurolophids through a complex pattern of evolutionary and growth-related changes. The edentulous region grew longer relative to dentary length, allowing for food acquisition specialization anteriorly and processing posteriorly, and became ventrally directed, possibly associated with foraging low-growing vegetation, especially in younger individuals. The saurolophid coronoid process became anteriorly

directed and relatively more elongate, with an expanded apex, increasing moment arm length, with muscles pulling the jaw more posteriorly, increasing mechanical advantage. During growth, all hadrosauroids underwent anteroposterior dental battery elongation by the addition of teeth, and edentulous region ventralization decreased. The dental battery became deeper in saurolophids by increasing the number of teeth per tooth family. The increased coronoid process anterior inclination and relative edentulous region elongation in saurolophids are hypothesized to have evolved through hypermorphosis and/or acceleration, peramorphic heterochronic processes; the development of an anteroposteriorly shorter but dorsoventrally taller saurolophid dentary, is probably due to post-displacement in dental battery elongation and edentulous region decreased ventral orientation, a paedomorphic heterochronic process.

**Key words:** hadrosaur, dentary, geometric morphometrics, heterochrony, paedomorphosis, peramorphosis.

HADROSAUROIDEA (*sensu* Sereno 1998) were Cretaceous high-fibre herbivores capable of processing their food through mastication (Weishampel 1983; Norman & Weishampel 1985; Weishampel & Norman 1989; Horner *et al.* 2004). Mastication is the process by which food is mechanically broken down into smaller particles, increasing the surface area available for chemical digestion. Extant vertebrates lack the enzymes to break down plant cell walls, instead utilizing mastication, along with symbiotic relationships with micro-organisms, to increase their ability to meet metabolic demands. As a result, the evolution of mastication in the past would have facilitated more efficient fermentation of plant cell walls and decreased the energy-cost of herbivory as a foraging

strategy (Norman & Weishampel 1985; Reilly *et al.* 2001; Ósi & Weishampel 2009; Tanoue *et al.* 2009; Ósi *et al.* 2014; Varriale 2016).

Mastication has long been thought of as a primarily mammalian feature and rare among other animals (Hildebrand 1937; Turnbull 1970; Herring *et al.* 2001). However, the fossil record has revealed this feeding process in several other vertebrate groups, such as in non-mammalian synapsids (Edaphosauridae and Dicynodontia), parareptiles (Procolophonia and Bolosauridae) and archosaurs (Ceratosauridae, Ankylosauria, Ornithomimidae, and the eusuchian *Iharkutosuchus*) (Norman & Weishampel 1985; Reilly *et al.* 2001; Ósi & Weishampel 2009; Tanoue *et al.* 2009; Ósi *et al.* 2014; Varriale 2016). Of

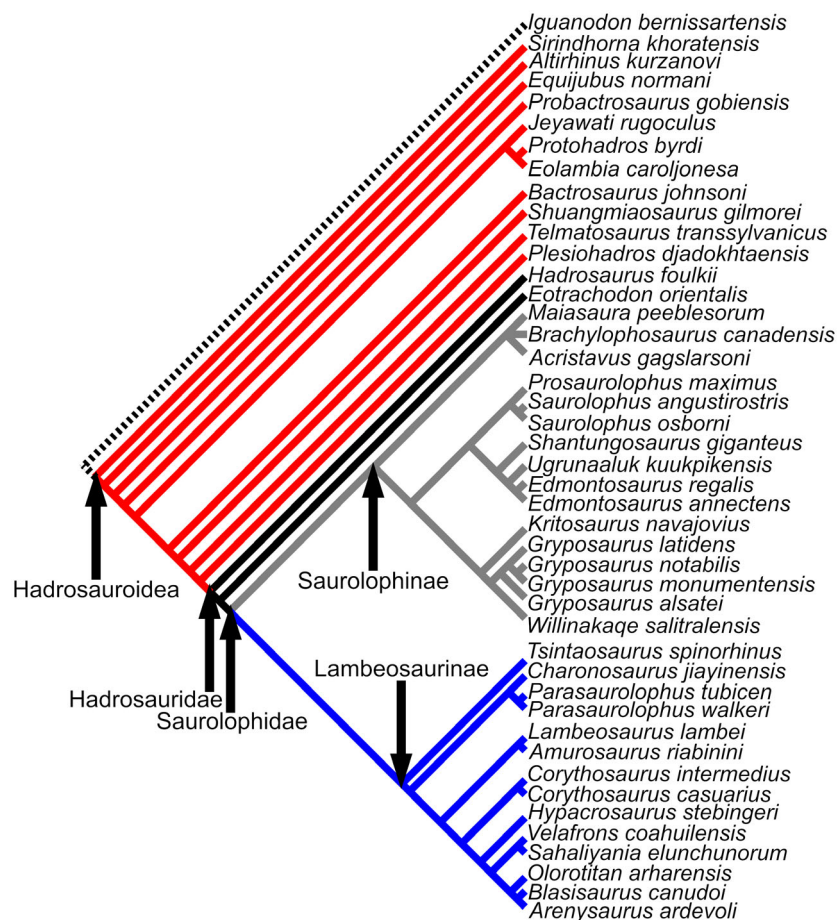


**FIG. 1.** Taxonomic and phylogenetic scheme used herein, based largely on that of Prieto-Márquez *et al.* (2016) and additional sources (see text). Outgroup taxon is *Iguanodon bernissartensis* (dashed line). Non-hadrosaurid hadrosauroids are indicated in red; non-saurolophid hadrosaurids in black; saurolophines in grey; lambeosaurines in blue.

these, duck-billed dinosaurs, or Hadrosauridae, evolved a highly derived dental organization that approached the complexity of extant grazing mammals (Norman & Weishampel 1985; Janis & Fortelius 1988; Carrano *et al.* 1999; Erickson *et al.* 2012; LeBlanc *et al.* 2016; Bramble *et al.* 2017).

Hadrosaurids, and the grade of taxa more closely related to them than to *Iguanodon* (Hadrosauroidae; Fig. 1), appeared during the Early Cretaceous (Aptian) of Asia (You *et al.* 2003; Norman 2014; Shibata *et al.* 2015) and reached a near-global distribution, before going extinct at the end of the Cretaceous (Case *et al.* 2000; Horner *et al.* 2004; Fanti *et al.* 2016). Their success is often attributed to a highly efficient masticatory apparatus that evolved progressively through several modifications of the hadrosauroid skull (Fig. 2) (Weishampel 1984; Norman & Weishampel 1985; Erickson *et al.* 2012; Stubbs *et al.* 2019). One of the skeletal elements modified in this manner was the dentary, a major constituent of the hadrosauroid lower jaw. Modifications pertaining to the dentary in the

transition from non-hadrosaurid hadrosauroids to Saurolophidae (= Lambeosaurinae + Saurolophinae, the two major clades of hadrosaurids) (Fig. 1) included: (1) an anteroposteriorly more elongate edentulous region relative to the length of the dentary, which separated regions of the mouth, allowing for increased specialization of food gathering (pre-dentary and premaxilla) and processing (dental battery) regions; (2) dorsoventral deepening of the dental battery by the addition of extra tooth rows, which allowed teeth and dental ligaments to work as shock absorbers during mastication; (3) posterior elongation of the dental battery medially past the coronoid process by the addition of more teeth to each row, which enlarged the grinding surface and increased leverage (increasing bite force); (4) teeth that interlocked more closely; (5) a functional tooth row in which nerves and blood vessels filled with dentine before erupting, allowing entire teeth to be completely ground down during mastication without interruption to food intake; and (6) dorsoventral elongation and an increased anterior angle of the coronoid process whose apex became

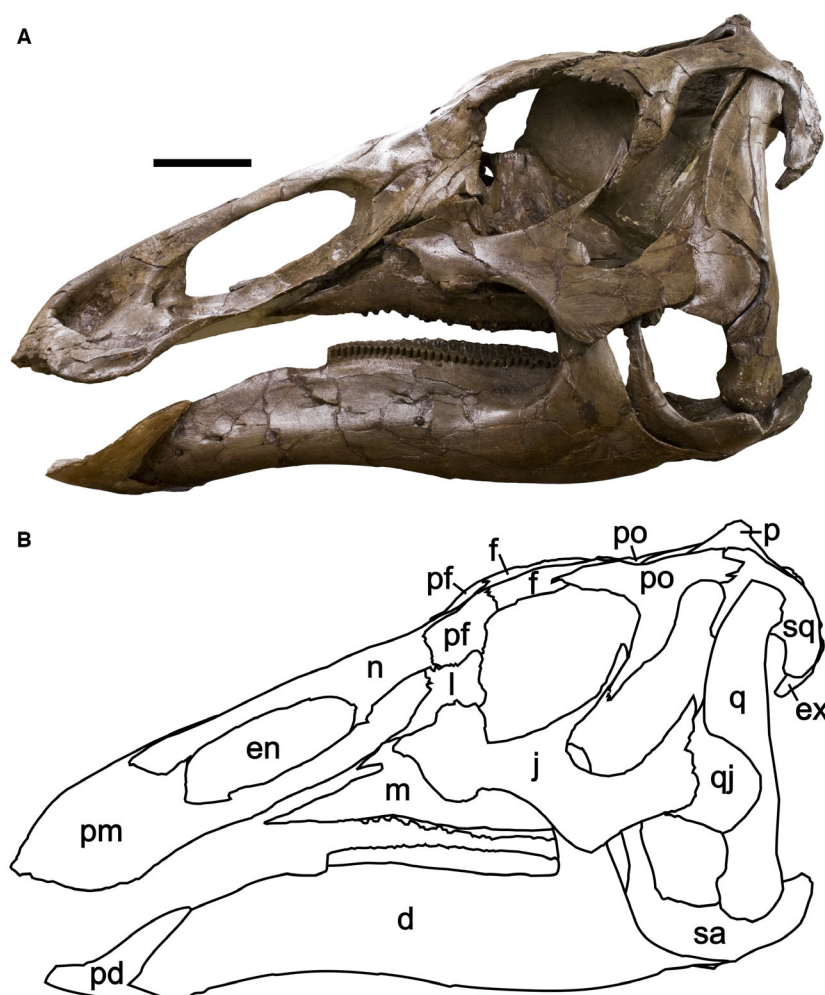


**FIG. 2.** Hadrosauroid skull anatomy exemplified by *E. annectens* CMN 8509 (holotype of *Edmontosaurus saskatchewanensis*) in left lateral view. A, photograph. B, interpretative line drawing. *Abbreviations:* d, dentary; en, external naris; ex, exoccipital–opisthotic complex; f, frontal; j, jugal; l, lacrimal; m, maxilla; n, nasal; p, parietal; pd, prementary; pf, prefrontal; pm, premaxilla; po, postorbital; q, quadrate; qj, quadratojugal; sa, surangular; sq, squamosal. Scale bar represents 10 cm.

expanded, increasing the surface area available for muscle attachment, further increasing leverage (Kubota & Kobayashi 2009; Evans 2010; Prieto-Márquez 2010; Norman 2014; Blanco *et al.* 2015; LeBlanc *et al.* 2016; Nabavizadeh 2016; Bramble *et al.* 2017) (Fig. 3A, B). These changes may have taken place in a single burst, due to increased rates of mandibular phenotypic evolution at the base of the saurolophid clade, followed by comparatively low rates of change in both Saurolophinae and Lambeosaurinae (Stubbs *et al.* 2019).

Feeding mechanics in hadrosauroids have long been discussed (e.g. Ostrom 1961). The pleurokinetic model (Fig. 4A) was favoured for over two decades (Norman 1984; Weishampel 1984; Norman & Weishampel 1985; Weishampel & Norman 1989). Pleurokinesis involves the elevation of the lower jaw, bringing the teeth of the

dentaries and maxillae into occlusion, pushing the maxillary teeth dorsolaterally, and rotating several cranial elements laterally along joints between the maxilla and premaxilla, maxilla–jugal and lacrimal, prefrontal and lacrimal, jugal and postorbital, quadrate and quadratojugal, basiptyergoid and pterygoid, as well as quadrate and squamosal (the pleurokinetic joint, *sensu* Weishampel 1984; Norman & Weishampel 1985). Although traditionally favoured, pleurokinesis is hindered by the morphology and position of the intracranial joints and the necessity for unlikely secondary displacements between several cranial elements, such as between the jugal and postorbital and the pterygoid and quadrate (Rybczynski *et al.* 2008; Cuthbertson *et al.* 2012). In an alternative model (Fig. 4B), the upper part of the skull is largely akinetic and, as the lower jaw is elevated and the teeth occlude, the lower jaw is

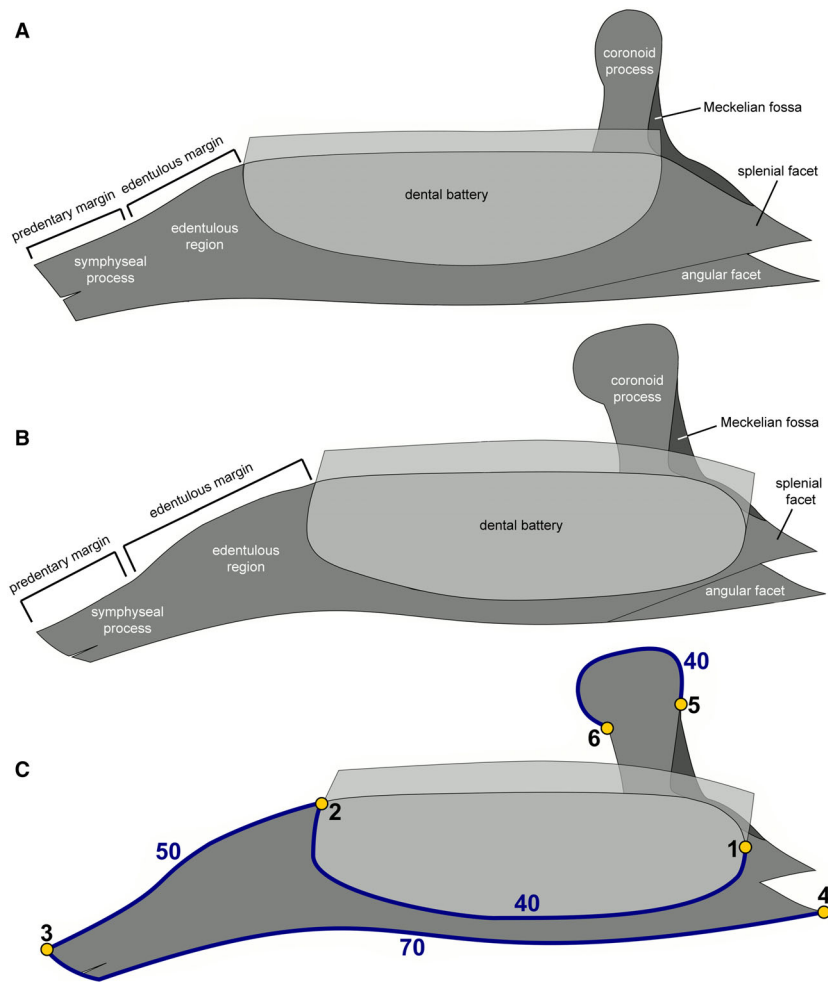


**FIG. 3.** Schematic, terminology, and digitization of hadrosauroid dentaries. A, schematic of an adult non-hadrosauroid hadrosauroid dentary. B, schematic of an adult saurolophid dentary. C, landmark configuration used in this study; dark blue lines represent curves digitized using sliding semilandmarks; the number of semilandmarks per curve is shown in dark blue; yellow points mark the ends of the curves, depicting fixed homologous landmarks (landmark numbers in black); for further landmark details, see Table 1.

simultaneously retracted and rotated along an axis parallel to the dentary (Cuthbertson *et al.* 2012; Nabavizadeh 2014). This model does not require complex displacements between cranial bones and follows tooth-wear patterns more closely than pleurokinesis (Nabavizadeh 2016). Importantly, this model emphasizes the lower jaw as a major module in the evolution of the hadrosauroid masticatory apparatus. Reconstructing its variation, specifically that of the dentary, as well as understanding its taxonomic and ontogenetic variation provides an important context to discuss the development of the hadrosauroid skull and the evolution of high-fibre herbivory in a non-mammalian system.

Understanding variation in the dentary will also improve our ability to construct, revise and interpret phylogenetic characters. For instance, characters related to the dentary can amount to *c.* 10% of the dataset (39/346

(11.3%) in Xing *et al.* 2017, supp. info.; 24/286 (8.4%) in Gates *et al.* 2021, supp. info.; 17/203 (8.4%) in McDonald *et al.* 2021, supp. info.; 26/283 (9.2%) in Prieto-Márquez & Carrera Farias 2021, supp. file). As a result, variation in the dentary imposes a great deal of influence on phylogenetic results, emphasizing the need for a more detailed quantitative examination of variation, in particular that associated with growth and size. Understanding the influence of non-taxonomic sources of variation enables the construction of more phylogenetically informative characters that hopefully reduce the amount of character conflict, increasing phylogenetic resolution.

This study investigates taxonomic, ontogenetic and individual variation in hadrosauroid dentary morphology (Fig. 2). We expect that the results will show morphological changes in the dentary that amount to more effective masticatory abilities, based on previous observations

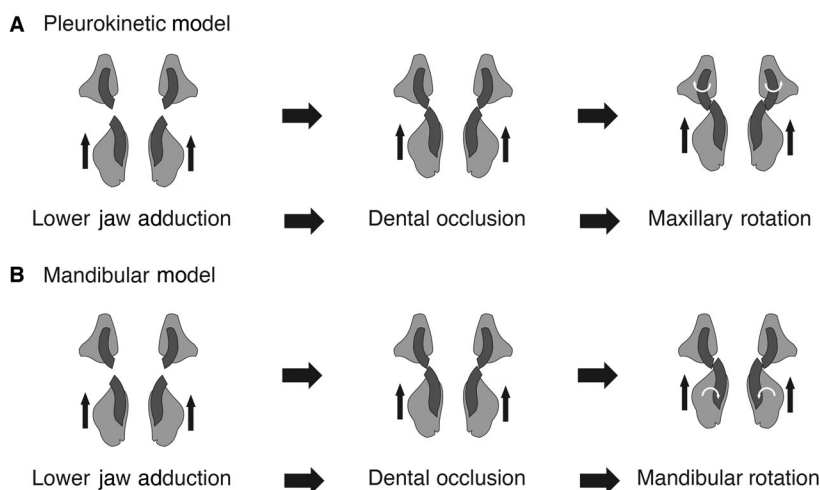


**FIG. 4.** The two hadrosauroid jaw-mechanic mastication models. A, pleurokinesis in cross-sectional view. B, alternative mastication model in cross-sectional view. All images based on those of Lambe (1920) and Nabavizadeh (2014) and show maxillae (above, light grey) and dentaries (below, light grey), with dental batteries (dark grey).

**TABLE 1.** Locations of the homologous landmarks at the ends of semilandmark curves (Fig. 3C).

No	Explanation
1	Posteriormost point of the dental battery.
2	Anteriormost point of the dental battery.
3	Anteriormost point of the symphyseal process.
4	Posteriormost point of the angular facet.
5	Intersection of the Meckelian fossa and the base of the anteroposteriorly expanded region of the coronoid process.
6	Anterior base of the anteroposteriorly expanded region of the coronoid process.

(Weishampel 1984; Norman & Weishampel 1985; Kubota & Kobayashi 2009; Norman 2014; LeBlanc *et al.* 2016; Nabavizadeh 2016; Nabavizadeh & Weishampel 2016). Additionally, previous research has shown that various aspects of dentary morphology in hadrosauroid taxa vary throughout ontogeny, a pattern that should also be detected here (Maryańska & Osmólska 1981; Kirkland 1998; Godefroit *et al.* 2004; Kubota & Kobayashi 2009; Bell 2011; Campione & Evans 2011; Prieto-Márquez 2011; McGarrity *et al.* 2013; Prieto-Márquez 2014; LeBlanc *et al.* 2016; Prieto-Márquez & Gutarra 2016; Bramble *et al.* 2017).

## MATERIAL AND METHOD

### Taxonomic nomenclature

The taxonomic scheme followed herein is largely based on Prieto-Márquez *et al.* (2016), with the addition of taxa that

were not included in their analysis from other literature sources. These include *Sirindhorna khoratensis* and *Altirhinus kurzanovi* (Shibata *et al.* 2015), *Shuangmiaosaurus gilmorei* (Xing *et al.* 2014), *Plesiohadros djadokhtaensis* (Tsongbaatar *et al.* 2014), *Ugrunaaluk kuukpikensis* (Mori *et al.* 2016), *Gryposaurus alsatei* (Lehman *et al.* 2016) and *Amurosaurus riabinini* (Xing *et al.* 2017) (Fig. 1).

Several of the taxonomic definitions used by Prieto-Márquez *et al.* (2016) are redefinitions of the previous nomenclature, based on a character matrix originally used by Prieto-Márquez in an earlier publication (Prieto-Márquez 2010, appendix). Hadrosauroidae is defined as *Hadrosaurus foulkii* Leidy, 1858, and every taxon more closely related to it than *Iguanodon bernissartensis* Boulenger, 1881 (*sensu* Prieto-Márquez 2010). Hadrosauridae is defined as the node representing the most recent common ancestor of *Parasaurolophus walkeri* Parks, 1922, and *Hadrosaurus foulkii* (*sensu* Prieto-Márquez 2010) and all of its descendants. In this tree, Hadrosauridae includes *Hadrosaurus foulkii*, *Eotrachodon orientalis* and Saurolophidae. Likewise, Saurolophidae (*sensu* Prieto-Márquez 2010) is defined as the most recent common ancestor of *Lambeosaurus lambei* Parks, 1923, and *Saurolophus osborni* Brown, 1913, and all of its descendants. Saurolophidae is divided into Saurolophinae and Lambeosaurinae. Saurolophinae (*sensu* Prieto-Márquez 2010) is defined as the stem that includes *Saurolophus osborni* and all taxa more closely related to it than to *Lambeosaurus lambei* or *Hadrosaurus foulkii*. Lambeosaurinae (*sensu* Prieto-Márquez 2010) is defined as the stem that includes *Lambeosaurus lambei* and all taxa more closely related to it than to *Edmontosaurus regalis* Lambe, 1917, *Saurolophus osborni*, or *Hadrosaurus foulkii*.

### Data collection

Images of hadrosauroid dentary specimens in medial view along with information on image source, taxonomic affinity, and ontogenetic stage (juvenile, subadult, or adult) were obtained from the literature and personal digital libraries (Appendix S1 and dataset reference list in Appendix S2). The dentary sample consisted of 84 specimens spanning at least 36 species. Seventy-four of the specimens were assigned to species level, and the remaining ten were assigned only to genus level. We used medial views of the dentaries because it is the view that exposes the greater number of characters and structures, such as the depth and extent of the dental battery, tooth crowns (when exposed upon removal of the dental lamina), the Meckelian fossa, and articular facets for bones like the splenial and angular (Fig. 3). The included specimens were well-preserved, including complete coronoid processes, outline of the dental batteries, and symphyseal processes. In a few examples, some of these structures were weathered or incomplete. Fortunately, these were insignificant to the extent of not preventing the appreciation of the actual morphology. Ontogenetic stage was primarily based on the literature pertaining to the digitized specimen. However, if such information was not provided, it was inferred based on the relative development of the crest (if present), or by comparing the size of the dentary following Evans (2010). Evans (2010) proposed an arbitrary division of ontogenetic stages into juvenile, subadult or adult if the individual skull length is <50%, 50–85%, or >85%, respectively, of the maximum skull length observed in that taxon. Taxa known from a single dentary that was not assigned to a particular ontogenetic stage were assumed to be adults due to the absence of comparative specimens, unless they could be compared with a closely related taxon of similar size.

*Institutional abbreviations.* AMNH, American Museum of Natural History, New York, USA; CMN, Canadian Museum of Nature, Ottawa, Canada; MOR, Museum of the Rockies, Bozeman, Montana, USA; MPC, Mongolian Paleontology Centre, Ulan Baatar, Mongolia; ROM, Royal Ontario Museum, Toronto, Ontario, Canada; TMP, Royal Tyrrell Museum of Paleontology, Drumheller, Alberta, Canada; UCMP, University of California Museum of Paleontology, Berkeley, California, USA.

### Digitization

Images of specimens were compiled into a TPS file in tpsUtil v1.74 (Rohlf 2017a) and digitized in tpsDIG2 v2.17 (Rohlf 2017b) following a semilandmark configuration designed to efficiently capture the highly curved morphology of the hadrosauroid dentary, yet still allow for as many specimens as possible to be included (see

Fig. 3C and Table 1 for a rationale of semilandmark placement). The angular and splenial facets at the posterior end of the dentary tend to be thin and often break off. Therefore, it was decided not to include the posterior margin in the digitization process, allowing specimens with missing angular and splenial facets to be included, and maximizing the sample size. Efforts were made to include the ventral edge of the angular facet. The positions of missing semilandmarks along the posteroventral edge were approximated by hand, based on comparisons with other specimens of the same species and ontogenetic stage, and only if those were deemed well preserved. Semilandmarks were resampled to a predetermined number of equidistant points that describe the curve. The semilandmarks were also scaled relative to their associated scale factor, calculated as the ratio of pixels per unit of distance as determined by the scale bar (e.g. centimetre) (Fig. 3C). The scaled semilandmarks were then used to calculate the centroid size of each specimen, a proxy for the overall size of the dentary.

### Generalized Procrustes and sliding semilandmark analyses

Digitized specimens were standardized relative to each other using a generalized Procrustes analysis (GPA), which removes or minimizes the influence of isometric size, position, and rotation, leaving only the shape-related variation in the data. During the GPA, semilandmarks were slid along the curves; their positions were determined by minimizing bending energies (Bookstein *et al.* 2002). In total, the analysis used 192 sliding semilandmarks and eight fixed landmarks at six homologous points (see Söderblom *et al.* 2023; Fig. 3C; Table 1). By sliding the semilandmarks, the variation in the arbitrary placement of individual semilandmarks was removed, shifting the assumed homology to the curve rather than the specific points (Bookstein *et al.* 2002). The generalized Procrustes analysis was run in R v4.1.3 (R Core Team 2013), using the package geomorph v3.2.1 (Adams & Otárola-Castillo 2013).

### Statistical analyses

All statistical analyses were run in R v4.1.3 (R Core Team 2013). Shape variation following GPA-alignment was assessed using a principal component analysis (PCA). The vast majority of interpretable variation was stored along PC1 and PC2 (Appendix S3), although other axes were examined for any apparent patterns. The proportions of variance explained by each PC axis were plotted onto corresponding PCs in the morphospace diagram. Thin-plate spline (TPS) grids of the shape described along

**TABLE 2.** Significance (p-value) obtained from Shapiro–Wilk normality tests on groupings by taxonomy, as well as taxonomy and ontogenetic stage combined for PC1 and PC2.

Group	PC1 p-value	PC2 p-value
Nonhad	0.738	<b>0.043</b>
Nonhad including <i>Eotrachodon orientalis</i>	0.507	0.066
Lam	0.182	0.557
Sau	0.273	0.057
Sau excluding AMNH 5730	0.580	0.050
Nonhad juveniles	0.781	0.431
Nonhad subadults	0.262	0.997
Nonhad subadults including <i>Eotrachodon orientalis</i>	0.253	0.970
Nonhad adults	0.268	0.482
Lam subadults	0.424	0.339
Lam adults	0.172	0.299
Sau juveniles	0.997	0.254
Sau subadults	0.402	0.101
Sau adults	0.222	0.500
Sau adults excluding AMNH 5730	0.160	0.669

Nonhad, non-hadrosaurid hadrosauroid; Lam, lambeosaurine; Sau, saurolophine.

All p-values rounded to three decimal places. Significant p-values ( $p < 0.05$ ) are in **bold**.

an axis reflect the minima and maxima in morphospace, and a consensus TPS grid reflects the average landmark configuration along all axes of variance. Density plots of the distributions along individual PCs reflect taxonomy (non-hadrosaurid hadrosauroids, lambeosaurines or saurolophines) split into ontogenetic stages (juvenile, subadult or adult) to provide further clarification of within-group and between-group variation. All reported statistical results have been rounded to three decimal places in the following discussion; accurate values are provided in Appendix S4 and Appendix S5.

Shapiro–Wilk normality tests and quantile–quantile (Q–Q) plots were used to determine the suitability of conducting parametric tests on the taxonomic and ontogenetic groupings of the sample. Almost all tests failed to reject normality (Table 2), except for non-hadrosaurid hadrosauroids along PC2 ( $W = 0.877$ ,  $p = 0.043$ ), and Q–Q plots show strong correlation, with few outliers (all correlation coefficients  $\geq 0.95$ ; the only exception ( $r = 0.9457$ ) occurred when *Eotrachodon* was excluded from non-hadrosaurid hadrosauroids along PC2; see Fig. S1). On these bases, standard parametric analyses of variance (ANOVA) and Tukey’s honest significant difference (TukeyHSD) tests were carried out on PC1 and PC2, which compared mean values of groups, divided both according to taxonomy and ontogenetic stage, and tested for significant differences. All p-values were adjusted for

multiple comparisons, using the default approach implemented in the TukeyHSD function. In addition to the default division of specimens into groups, the ANOVA and TukeyHSD tests were re-run twice. The first, excluding the *Edmontosaurus annectens* specimen AMNH 5730 (holotype of *Anatotitan copei*), as its position along PC1 supports previous interpretations that it might be dorsoventrally crushed (Campioni & Evans 2011). The second, considering *Eotrachodon orientalis* as a non-hadrosaurid hadrosauroid to test the effects of its different taxonomic placement on the results (see Xing *et al.* 2017). Normality tests following the removal of AMNH 5730 or when altering the taxonomic assignment of *E. orientalis* failed to reject normality along PC1 or PC2 for either Saurolophinae or non-hadrosaurid hadrosauroids, respectively (PC1:  $W = 0.976$ ,  $p = 0.580$  and  $W = 0.951$ ,  $p = 0.507$ ; PC2:  $W = 0.942$ ,  $p = 0.050$  and  $W = 0.895$ ,  $p = 0.066$ ).

A trajectory analysis, whereby the geometric attributes of phenotypic trajectories are compared pairwise (Collyer & Adams 2013), was run on the three aforementioned taxonomic and ontogenetic groups to quantify and visualize general shape changes, using the R package RRPP v1.3.1 (Collyer & Adams 2018, 2019). Additionally, growth-related changes were analysed via several bivariate linear models using natural logarithm centroid size (a proxy for dentary size, body size and growth stage) and PCs. Linear models serve as a more continuous assessment of growth rather than defining somewhat arbitrary growth classifications. Unfortunately, not all images analysed here included a scale bar and were thus excluded from the allometry plots. As some species are known only from a few specimens, plots were generated at the genus level to maximize sample size. Accordingly, all results should be interpreted as general growth patterns that approximate but are not species-specific ontogenetic trajectories. Linear models were used to test for allometry, whereby a slope coefficient statistically different from zero (i.e. significant) indicates allometry, whereas a non-significant result suggests the pattern cannot reject isometry. Large-scale clade/grade linear models and tests for allometry were also generated to further elucidate general growth patterns. Linear models are based on a standardized major axis (SMA) estimation of slope and intercept confidence intervals, implemented using the `sma()` function in the R package `smatr` v3.4-8 (Warton *et al.* 2012).

Finally, Mori *et al.* (2016) named a new saurolophid species, *Ugrunaaluk kuukpikensis*, based on juvenile specimens previously classified as *Edmontosaurus* sp. (Gangloff & Fiorillo 2010). This taxonomic interpretation has since been contested by independent authors (Xing *et al.* 2017; Takasaki *et al.* 2020), who support a more conservative *Edmontosaurus* sp. designation for these specimens, pending the discovery of adult individuals. Nonetheless, to provide further insights into the validity of the dentary

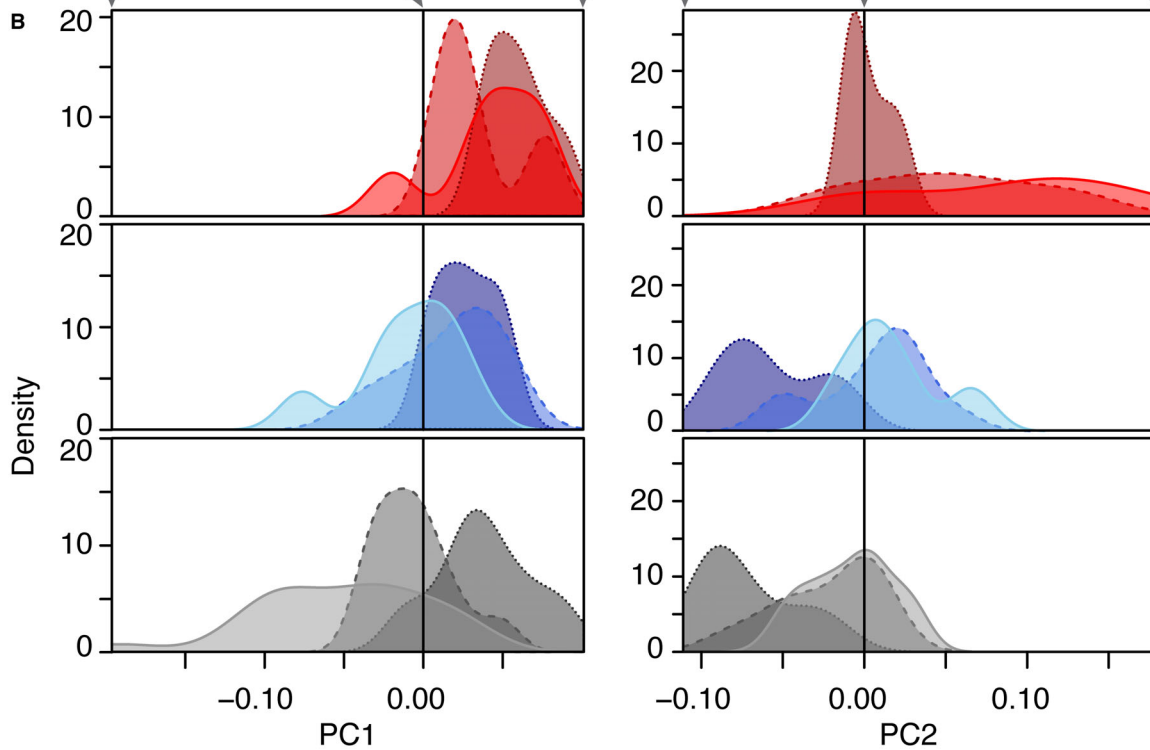
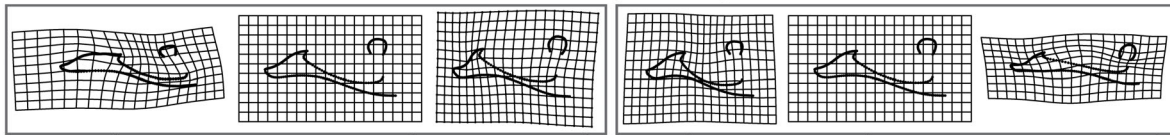
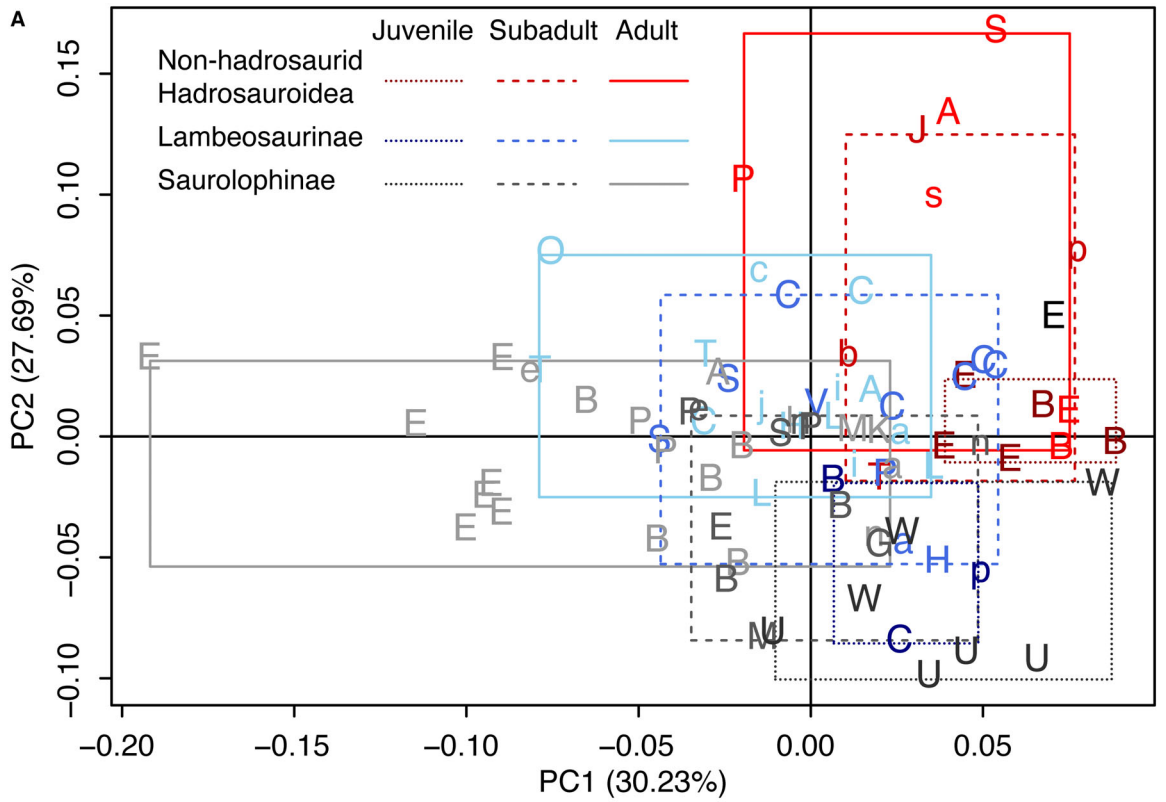




**FIG. 5.** Morphospace along principal components 1 and 2. A, bivariate plot between PC1 and PC2; boxes show minimum and maximum extents of each group along respective principal components. B, density plots depict the distribution of each taxonomic and ontogenetic grouping along PC1 and PC2 separately; thin-plate spline grids display aspects of morphology that change along axes. Major taxonomic groups divided by colour (red, blue and grey shades); ontogenetic stages (juvenile, subadult and adult) are divided by shade (dark, medium and light, respectively) and line type (dotted, dashed and solid, respectively). Black lines mark zero along principal component axes in bivariate and density plots. Taxa plotted on A: **non-hadrosaurid hadrosauroids** (red): A, *Altirhinus kuzanovi*, B, *Bactrosaurus johnsoni*; E, *Eolambia caroljonesa*; J, *Jeyawati rugoculus*; P, *Plesiohadros djadokhtaensis*; p, *Probactrosaurus gobiensis*; b, *Protohadros byrdi*; S, *Shuangmiaosaurus gilmorei*; s, *Sirindhorna khoratensis*; T, *Telmatosaurus transsylvanicus*; **non-saurolophid hadrosaurid** (black): E, *Eotrachodon orientalis*; **lambeosaurines** (blue): A, *Arenysaurus ardevoli*; a, *Amurosaurus riabinini*; B, *Blasisaurus canudoi*; j, *Charonosaurus jiayinensis*; c, *Corythosaurus casuarius*; i, *Corythosaurus intermedius*; C, *Corythosaurus* sp.; H, *Hypacrosaurus stebingeri*; L, *Lambeosaurus lambei*; O, *Olorotitan arharensis*; P, *Parasaurolophus tubicen*; p, *Parasaurolophus* sp.; S, *Sahaliyana elunchunorum*; T, *Tsintaosaurus spinorhinus*; V, *Velafrons coahuilensis*; **saurolophines** (grey): A, *Acristavus gagslarsoni*; B, *Brachylophosaurus canadensis*; E, *Edmontosaurus annectens*; e, *Edmontosaurus regalis*; a, *Gryposaurus alsatei*; l, *Gryposaurus latidens*; n, *Gryposaurus notabilis*; G, *Gryposaurus* sp.; K, *Kritosaurus navajovius*; M, *Maiasaura peeblesorum*; P, *Prosaurolophus maximus*; S, *Saurolophus angustirostris*; U, *Ugrunaaluk kuukpikensis*; W, *Willinakaqe salitralensis*.

characters that define *U. kuukpikensis* and to investigate potential differential dentary growth patterns involving *Edmontosaurus* and *Ugrunaaluk*, a separate linear model combining *U. kuukpikensis* and *Edmontosaurus* as one taxon was generated and tested against all other regressions at the generic level through SMA estimation of slope confidence intervals.

## RESULTS

### Morphospace

Only PC1 and PC2 showed significant patterns between taxonomic and ontogenetic groups of interest. Neither PC3 (c. 13% of the total variance) nor PC4 (c. 6%) revealed any notable variance (Appendix S3; Fig. S2). Accordingly, we focus on the first two axes in the subsequent analysis.

*Principal component 1.* PC1 represents 30.23% of the total variance in the sample and depicts the variation in the inclination of the coronoid process, the size of the coronoid process' apex, and the relative length of the edentulous region (Fig. 5). Specimens on the negative end of PC1 have an anteriorly inclined coronoid process with a large apex and an elongated edentulous region, whereas those on the positive end of PC1 have an increasingly more dorsally inclined coronoid process with a smaller apex and a shortened edentulous region. Within this context, non-hadrosaurid hadrosauroids load positively along PC1, except for *Plesiohadros djadokhtaensis* (MPC-D100/745). The saurolophids (lambeosaurines and saurolophines) also load positively along PC1 but, unlike non-hadrosaurid hadrosauroids, specimens explore the negative regions along the axis even further. Saurolophines show the most extreme negative condition along

PC1, independent of whether AMNH 5730 (a negative outlier along PC1) is ignored. The separation in morphospace occupation between non-hadrosaurid hadrosauroids and saurolophids (saurolophines and lambeosaurines) is quantitatively supported by all ANOVA and TukeyHSD tests ( $p \leq 0.022$ ; Table 3; Appendix S4), independently of whether *Eotrachodon orientalis* is included as a non-saurolophid hadrosaurid (four groups) or non-hadrosaurid hadrosaurid (three groups), or whether AMNH 5730 is excluded (Table 3). Saurolophines and lambeosaurines can only be statistically differentiated from each other if *E. orientalis* is included as a non-hadrosaurid hadrosaurid (three-group analysis) and AMNH 5730 is included. Following a similar pattern as the four-group TukeyHSD test, the trajectory analysis (Fig. 6) shows a separation of non-hadrosaurid hadrosaurid and saurolophid mean value extents (the extent of the circles connected by lines) as well. However, lambeosaurines and saurolophines overlap in the extent of their mean values in the trajectory analysis.

The morphospace plot and trajectory analysis emphasize the growth trajectory along PC1, with ranges and mean values of juveniles loading more positively, subadults intermediately (however with an extensive overlap with juveniles in lambeosaurines), and adults more negatively, which hints at a growth-dependent change in average morphology (Figs 5, 6A–B). Saurolophids display more morphological change, on average, when transitioning from juvenile to subadult growth stages than when transitioning from subadult to adult stages. The same pattern is visible in the average values for the non-hadrosaurid hadrosaurid growth stages, although it is less pronounced.

All ANOVA tests run with the sample divided by taxonomy and ontogeny recovered significant differences ( $F = 8.653$ ;  $p < 0.001$ ), independent of the status of *Eotrachodon* ( $F = 9.674$ ;  $p < 0.001$ ), the exclusion

**TABLE 3.** Significance (p-value adjusted for multiple comparisons) obtained from Tukey's honest significant difference tests grouped by taxonomy for PC1.

	Default	Excluding AMNH 5730	<i>Eotrachodon</i> as Nonhad	Excl. AMNH 5730, and <i>Eotrachodon</i> as Nonhad
Nonhad – Lam	<b>0.022</b>	<b>0.01</b>	<b>0.007</b>	<b>0.003</b>
<i>Eotrachodon</i> – Lam	0.468	0.385		
Sau – Lam	0.085	0.137	<b>0.047</b>	0.079
<i>Eotrachodon</i> – Nonhad	0.952	0.938		
Sau – Nonhad	<b>&lt; 0.001</b>	<b>&lt; 0.001</b>	<b>&lt; 0.001</b>	<b>&lt; 0.001</b>
Sau – <i>Eotrachodon</i>	0.181	0.15		

Nonhad, non-hadrosaurid hadrosauroid; Lam, lambeosaurine; Sau, saurolophine.

Significant p-values ( $p < 0.05$ ) are in **bold**. All values reported here to three decimal places; detailed statistics can be found in Appendix S4.

of AMNH 5730 ( $F = 9.011$ ;  $p < 0.001$ ), or both combined ( $F = 10.036$ ;  $p < 0.001$ ) (Appendix S4). Overall, juveniles across all taxonomic groups exhibit similar morphologies along PC1 (Fig. 5), and no significant differences were recovered between these categories following the TukeyHSD test (Table 4). Furthermore, juvenile saurolophines display morphologies that overlap with almost the entire range of variation observed in the non-hadrosaurid hadrosauroid grade (including juveniles, subadults and adults) along PC1 and cannot be differentiated statistically from any of the non-hadrosaurid hadrosauroids growth-stages. Similar results were obtained between lambeosaurine juveniles and all non-hadrosaurid hadrosauroids (Table 4). Lambeosaurine subadults display a broader range of morphologies along PC1 than saurolophine subadults. Despite these apparent differences, subadult stages could not be differentiated from each other (Table 4).

The adult stages of all taxonomic groups partially overlap with each other. Nevertheless, saurolophine adults are significantly different from all taxonomic and ontogenetic categories, except for saurolophine subadults ( $p = 0.052$ ) and lambeosaurine adults ( $p = 0.057$ ), given their exploration of more negatively loaded morphologies along PC1 (Table 4). If *E. orientalis* is considered a non-hadrosaurid hadrosauroid and AMNH 5730 is included, the saurolophine adults become significantly different from the saurolophine subadults and the lambeosaurine adults as well. This result shows that saurolophines display the most extreme ontogenetic change along this PC axis (Fig. 5). Lambeosaurines display less ontogenetic change than saurolophines, as seen from the position and range of lambeosaurines along PC1 (Fig. 5) wherein no significant differences were found between stages (Table 4). Non-hadrosaurid hadrosauroids display even less ontogenetic change than lambeosaurines as seen from their position and range along PC1, and like lambeosaurines, their

morphology cannot be proven to significantly differ between stages. The most negatively extreme adult morphologies along PC1, with the most anteriorly inclined coronoid process and elongated edentulous region for each taxonomic group are exemplified by *Plesiohadros djadokhtaensis* (a non-hadrosaurid hadrosauroid), *Tsintaosaurus spinorhinus* and *Olorotitan arharensis* (lambeosaurines), and *Edmontosaurus* (a saurolophine genus). Additionally, lambeosaurine adults are significantly different from non-hadrosaurid hadrosauroid juveniles, and saurolophine adults are significantly different from both non-hadrosaurid hadrosauroid juveniles and subadults, while non-hadrosaurid hadrosauroid adults are not significantly different from juveniles and subadults of all three taxonomic groups (Table 4).

Removal of AMNH 5730 (a negative outlier along PC1) from the analyses results in minor changes to p-values, including that the non-hadrosaurid hadrosauroid juveniles become significantly different from saurolophine subadults ( $p = 0.024$ ) and *E. orientalis* can be differentiated from saurolophine adults ( $p = 0.048$ ). Inclusion of *E. orientalis* as a non-hadrosaurid hadrosauroid resulted in the following significant comparisons, which were not significant in the initial analysis: saurolophine adults and lambeosaurine adults ( $p = 0.047$ ); saurolophine subadults and non-hadrosaurid hadrosauroid juveniles ( $p = 0.050$ ); saurolophine subadults and saurolophine adults ( $p = 0.043$ ). When the analysis was run with *E. orientalis* as a non-hadrosaurid hadrosauroid and excluding AMNH 5730 (Table 4), the following comparisons became significant: non-hadrosaurid hadrosauroid adults and lambeosaurine adults ( $p = 0.048$ ); saurolophine subadults and non-hadrosaurid hadrosauroid juveniles ( $p = 0.020$ ).

*Principal component 2.* PC2 represents 27.69% of the total variance in the sample and describes variation in the

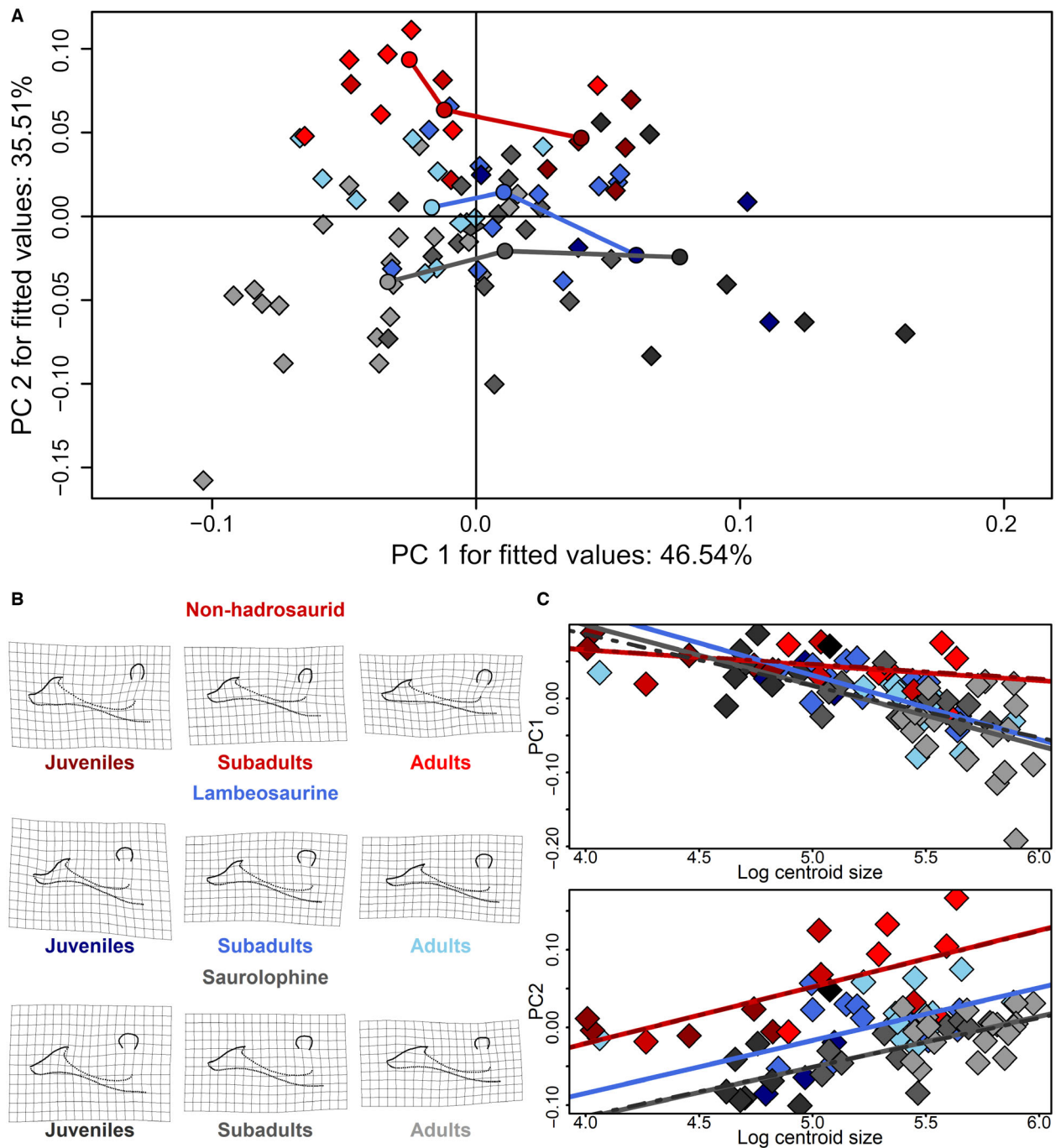


**FIG. 6.** Trajectory analysis and linear growth patterns across PC1 and PC2. A, trajectory analysis, taxonomic and ontogenetic colour palette as per Figure 5; each diamond represents a dentary, circles are the mean values along PC1 and PC2, given a taxonomic and ontogenetic group, and lines denote the trajectory from juvenile to adult. B, consensus thin-plate spline (TPS) grids of the average morphologies at the group means (i.e. circles in A). C, linear models, scaling PC1 and PC2 against log (natural logarithm) centroid size by clade/grade; line colours as per Figure 5, with the addition of a red dot-dashed line representing non-hadrosaurid hadrosauroids including *Eotrachodon orientalis*, and a grey dot-dashed line representing saurolophines excluding AMNH 5730.

dorsoventral elongation of the coronoid process compared to the length of the dentary, the relative dorsoventral depth of the dental battery, and the ventral angle of

the edentulous region relative to the main axis of the dentary (Fig. 5). Specimens on the negative end of PC2 have tall coronoid processes, dorsoventrally deep but

**TABLE 4.** Significance (p-value adjusted for multiple comparisons) obtained from Tukey's honest significant difference tests grouped by ontogenetic stage within taxonomic groups for PC1.

	Default	Excluding AMNH 5730	<i>Eotrachodon</i> as Nonhad	Excl. AMNH 5730, and <i>Eotrachodon</i> as Nonhad
Lam juv – Lam adu	0.859	0.773	0.817	0.724
Lam sub – Lam adu	0.712	0.583	0.658	0.529
Nonhad adu – Lam adu	0.123	0.058	0.103	<b>0.048</b>
Nonhad juv – Lam adu	<b>0.021</b>	<b>0.007</b>	<b>0.017</b>	<b>0.005</b>
Nonhad sub – Lam adu	0.548	0.404	0.187	0.101
<i>Eotrachodon</i> – Lam adu	0.556	0.412		
Sau adu – Lam adu	0.057	0.119	<b>0.047</b>	0.100
Sau juv – Lam adu	0.151	0.074	0.127	0.062
Sau sub – Lam adu	1	1	1	1
Lam sub – Lam juv	1	1	1	1
Nonhad adu – Lam juv	1	1	1	0.999
Nonhad juv – Lam juv	0.975	0.953	0.961	0.932
Nonhad sub – Lam juv	1	1	1	1
<i>Eotrachodon</i> – Lam juv	0.992	0.984		
Sau adu – Lam juv	<b>0.037</b>	<b>0.036</b>	<b>0.031</b>	<b>0.03</b>
Sau juv – Lam juv	1	1	1	1
Sau sub – Lam juv	0.942	0.897	0.917	0.863
Nonhad adu – Lam sub	0.944	0.900	0.919	0.866
Nonhad juv – Lam sub	0.556	0.412	0.501	0.364
Nonhad sub – Lam sub	0.999	0.998	0.959	0.928
<i>Eotrachodon</i> – Lam sub	0.939	0.893		
Sau adu – Lam sub	<b>&lt; 0.001</b>	<b>&lt; 0.001</b>	<b>&lt; 0.001</b>	<b>&lt; 0.001</b>
Sau juv – Lam sub	0.976	0.955	0.962	0.933
Sau sub – Lam sub	0.917	0.858	0.885	0.817
Nonhad juv – Nonhad adu	0.999	0.998	0.998	0.996
Nonhad sub – Nonhad adu	1	1	1	1
<i>Eotrachodon</i> – Nonhad adu	1	0.999		
Sau adu – Nonhad adu	<b>&lt; 0.001</b>	<b>&lt; 0.001</b>	<b>&lt; 0.001</b>	<b>&lt; 0.001</b>
Sau juv – Nonhad adu	1	1	1	1
Sau sub – Nonhad adu	0.274	0.160	0.236	0.136
Nonhad sub – Nonhad juv	0.991	0.982	0.998	0.995
<i>Eotrachodon</i> – Nonhad juv	1	1		
Sau adu – Nonhad juv	<b>&lt; 0.001</b>	<b>&lt; 0.001</b>	<b>&lt; 0.001</b>	<b>&lt; 0.001</b>
Sau juv – Nonhad juv	0.994	0.988	0.989	0.980
Sau sub – Nonhad juv	0.061	<b>0.024</b>	<b>0.050</b>	<b>0.020</b>
<i>Eotrachodon</i> – Nonhad sub	0.997	0.994		
Sau adu – Nonhad sub	<b>0.003</b>	<b>0.003</b>	<b>&lt; 0.001</b>	<b>&lt; 0.001</b>
Sau juv – Nonhad sub	1	1	1	1
Sau sub – Nonhad sub	0.737	0.614	0.353	0.229
Sau adu – <i>Eotrachodon</i>	0.068	<b>0.048</b>		
Sau juv – <i>Eotrachodon</i>	0.999	0.997		
Sau sub – <i>Eotrachodon</i>	0.651	0.514		
Sau juv – Sau adu	<b>&lt; 0.001</b>	<b>&lt; 0.001</b>	<b>&lt; 0.001</b>	<b>&lt; 0.001</b>
Sau sub – Sau adu	0.052	0.094	<b>0.043</b>	0.079
Sau sub – Sau juv	0.334	0.207	0.291	0.177

Nonhad, non-hadrosaurid hadrosauroid; Lam, lambeosaurine; Sau, Saurolophine; juv, juveniles; sub, subadults; adu, adults.

Significant p-values ( $p < 0.05$ ) are in **bold**. All values reported here to three decimal places; detailed statistics can be found in Appendix S4.

anteroposteriorly short dental batteries, and more ventrally oriented edentulous regions, whereas those on the positive end of PC2 have short coronoid processes,

dorsoventrally shallow but anteroposteriorly elongate dental batteries, and edentulous regions that are roughly in line with the main axis of the dentary. Non-hadrosaurid

**TABLE 5.** Significance (p-value adjusted for multiple comparisons) obtained from Tukey's honest significant difference tests grouped by taxonomy for PC2.

	Default	<i>Eotrachodon</i> as Nonhad
Nonhad – Lambeosaurinae	<b>0.01</b>	<b>0.004</b>
<i>Eotrachodon</i> – Lambeosaurinae	0.743	
Saurolophinae – Lambeosaurinae	<b>0.033</b>	<b>0.017</b>
<i>Eotrachodon</i> – Nonhad	1	
Saurolophinae – Nonhad	<b>&lt; 0.001</b>	<b>&lt; 0.001</b>
Saurolophinae – <i>Eotrachodon</i>	0.335	

Nonhad, non-hadrosaurid hadrosauroid.

Significant p-values ( $p < 0.05$ ) are in **bold**. All values reported here to three decimal places; detailed statistics can be found in Appendix S4.

hadrosauroids load positively along PC2, with the exception of some *Bactrosaurus* and *Eolambia* specimens, whereas saurolophines and lambeosaurines load either centrally or negatively along the axis, juvenile saurolophines being the most positively extreme condition (Fig. 5). Strong significant differences were recovered between non-hadrosaurid hadrosauroids and saurolophids ( $p < 0.01$ ; Table 5; Appendix S4) along with minor significant differences between saurolophines and lambeosaurines ( $p = 0.033$ ). When *E. orientalis* was treated as a non-hadrosaurid hadrosauroid, all comparisons became even more significant (Table 5).

When considering major growth stages, the ANOVA recovered overall significant differences along PC2 ( $F = 10.309$ ;  $p < 0.001$ ; Appendix S4). Juveniles tend to have lower PC2 values than older growth stages and, in general, the TukeyHSD test shows that juveniles are significantly different from their adult counterparts (non-hadrosaurid hadrosauroids:  $p = 0.009$ ; Lambeosaurinae:  $p = 0.039$ ; Saurolophinae:  $p = 0.003$ ; Table 6; Appendix S4). Juvenile saurolophines are significantly different from all non-hadrosaurid hadrosauroid ontogenetic stages and lambeosaurine subadults and adults, but are indistinguishable from lambeosaurine juveniles and saurolophine subadults along PC2 (Table 6). Lambeosaurine juveniles are separated from non-hadrosaurid hadrosauroids in morphospace and are significantly different from subadult and adult non-hadrosaurid hadrosauroids ( $p = 0.004$  and  $p < 0.001$ , respectively; Table 6). Non-hadrosaurid hadrosauroid juveniles are completely enveloped by their subadult, and partially by their adult, counterparts, with significant differences between the latter ( $p = 0.009$ ) but not the former ( $p = 0.541$ ).

Subadults load intermediately between the juveniles and adults (Fig. 5) and no significant differences were detected between the subadults and adults within any taxonomic group (Table 6). Of the subadult groups, saurolophines

load more negatively, non-hadrosaurid hadrosauroids load more positively, and lambeosaurines occupy an intermediate morphospace. Of these, only non-hadrosaurid hadrosauroid and saurolophine subadults can be differentiated from each other statistically ( $p = 0.015$ , Table 6). Non-hadrosaurid hadrosauroid subadults are also significantly different from both lambeosaurine ( $p = 0.04$ ) and saurolophine juveniles ( $p < 0.001$ ). Saurolophine subadults cannot be differentiated from non-hadrosaurid hadrosauroid adults ( $p = 0.065$ ); however, when *E. orientalis* is considered a non-hadrosaurid hadrosauroid this comparison becomes significant ( $p = 0.024$ ). Saurolophine subadults are indistinguishable from all other groups, including saurolophine juveniles ( $p = 0.129$ ) and adults ( $p = 0.981$ ). Lambeosaurine subadults are significantly different from the two most extreme groups in PC2 morphospace, the non-hadrosaurid hadrosauroid adults ( $p = 0.001$ ) and saurolophine juveniles ( $p < 0.001$ ), but are indistinguishable from all other groups, including lambeosaurine juveniles ( $p = 0.177$ ) and adults ( $p = 0.998$ ). The only non-saurolophid hadrosaurid in the sample, *E. orientalis*, loads positively and within the morphospace occupied by non-hadrosaurid hadrosauroids, as well as lambeosaurine subadults and adults (Fig. 5).

Saurolophid adults load centrally along PC2; saurolophines tend towards more negative values whereas lambeosaurines generally load more positively. Adult saurolophines are significantly different from non-hadrosaurid hadrosauroid adults and saurolophine juveniles (both  $p \leq 0.003$ ), but not other groups. Lambeosaurine adults are significantly different from non-hadrosaurid hadrosauroid adults ( $p = 0.006$ ), lambeosaurine juveniles ( $p = 0.039$ ), and saurolophine juveniles ( $p < 0.001$ ), but are indistinguishable from other groups, including lambeosaurine subadults ( $p = 0.998$ ). The non-hadrosaurid hadrosauroid adults load positively (with the exception of *Bactrosaurus*, which loads negatively), and are significantly different from all other taxonomic and ontogenetic groups, except for non-hadrosaurid hadrosauroid subadults ( $p = 0.915$ ). Overall, the two saurolophid clades have translated in a negative direction along PC2 compared to the position of the non-hadrosaurid hadrosauroid grade (Figs 5, 6C).

#### Size-related patterns

Line-fitting analysis linear slope coefficients could not be statistically differentiated from zero (Table 7; Appendix S5) and, as such, isometry cannot be rejected at the generic level along PC1 and PC2, with the exception of the combined *Edmontosaurus/Ugrunaaluk* analyses (Fig. 7H–J), where isometry is rejected in favour of allometry (PC1, AMNH 5730 included:  $p < 0.001$ , slope =  $-0.12149$ ,

**TABLE 6.** Significance (p-value adjusted for multiple comparisons) obtained from Tukey's honest significant difference tests grouped by ontogenetic stage within taxonomic groups for PC2.

	Default	<i>Eotrachodon</i> as Nonhad
Lam juveniles – Lam adults	<b>0.039</b>	<b>0.030</b>
Lam subadults – Lam adults	0.998	0.995
Nonhad adults – Lam adults	<b>0.006</b>	<b>0.005</b>
Nonhad juveniles – Lam adults	0.999	0.997
Nonhad subadults – Lam adults	0.752	0.614
<i>Eotrachodon</i> – Lam adults	0.997	
Sau adults – Lam adults	0.490	0.430
Sau juveniles – Lam adults	<b>&lt; 0.001</b>	<b>&lt; 0.001</b>
Sau subadults – Lam adults	0.127	0.103
Lam subadults – Lam juveniles	0.177	0.145
Nonhad adults – Lam juveniles	<b>&lt; 0.001</b>	<b>&lt; 0.001</b>
Nonhad juveniles – Lam juveniles	0.373	0.320
Nonhad subadults – Lam juveniles	<b>0.004</b>	<b>0.002</b>
<i>Eotrachodon</i> – Lam juveniles	0.23	
Sau adults – Lam juveniles	0.434	0.377
Sau juveniles – Lam juveniles	1	0.999
Sau subadults – Lam juveniles	0.891	0.851
Nonhad adults – Lam subadults	<b>0.001</b>	<b>&lt; 0.001</b>
Nonhad juveniles – Lam subadults	1	1
Nonhad subadults – Lam subadults	0.417	0.276
<i>Eotrachodon</i> – Lam subadults	0.973	
Sau adults – Lam subadults	0.986	0.976
Sau juveniles – Lam subadults	<b>&lt; 0.001</b>	<b>&lt; 0.001</b>
Sau subadults – Lam subadults	0.663	0.601
Nonhad juveniles – Nonhad adults	<b>0.009</b>	<b>0.007</b>
Nonhad subadults – Nonhad adults	0.915	0.822
<i>Eotrachodon</i> – Nonhad adults	0.995	
Sau adults – Nonhad adults	<b>&lt; 0.001</b>	<b>&lt; 0.001</b>
Sau juveniles – Nonhad adults	<b>&lt; 0.001</b>	<b>&lt; 0.001</b>
Sau subadults – Nonhad adults	<b>&lt; 0.001</b>	<b>&lt; 0.001</b>
Nonhad subadults – Nonhad juveniles	0.541	0.417
<i>Eotrachodon</i> – Nonhad juveniles	0.971	
Sau adults – Nonhad juveniles	1	0.999
Sau juveniles – Nonhad juveniles	<b>0.017</b>	<b>0.013</b>
Sau subadults – Nonhad juveniles	0.931	0.900
<i>Eotrachodon</i> – Nonhad subadults	1	
Sau adults – Nonhad subadults	0.065	<b>0.024</b>
Sau juveniles – Nonhad subadults	<b>&lt; 0.001</b>	<b>&lt; 0.001</b>

(continued)

**TABLE 6.** (Continued)

	Default	<i>Eotrachodon</i> as Nonhad
Sau subadults – Nonhad subadults	<b>0.015</b>	<b>0.005</b>
Sau adults – <i>Eotrachodon</i>	0.847	
Sau juveniles – <i>Eotrachodon</i>	0.056	
Sau subadults – <i>Eotrachodon</i>	0.629	
Sau juveniles – Sau adults	<b>0.003</b>	<b>0.002</b>
Sau subadults – Sau adults	0.981	0.968
Sau subadults – Sau juveniles	0.129	0.105

Nonhad, non-hadrosaurid hadrosauroid; Lam, lambeosaurine; Sau, saurolophine.

Significant p-values ( $p < 0.05$ ) are in **bold**. All values reported here to three decimal places; detailed statistics can be found in Appendix S4.

AMNH 5730 excluded:  $p < 0.001$ , slope =  $-0.10414$ ; PC2, AMNH 5730 included:  $p < 0.001$ , slope =  $0.08853$ , AMNH 5730 excluded:  $p < 0.001$ , slope =  $0.08475$ ). However, in the standardized major axis estimation, comparing the slopes of the different genera to one another, none could be differentiated statistically from each other (Table 8).

Significant patterns are more evident at the higher clade/grade level (Figs 6, 7; Tables 7–9). Along PC1, only the two saurolophid clades could be significantly differentiated from zero, and hence reject isometry in favour of allometry (lambeosaurines:  $p < 0.001$ , slope =  $-0.08703$ ; saurolophines, including AMNH 5730:  $p < 0.001$ , slope =  $-0.08159$ ; saurolophines, excluding AMNH 5730:  $p < 0.001$ , slope =  $-0.06995$ ). This was not the case in non-hadrosaurid hadrosauroids (Table 7; Appendix S5), indicating little or no change in coronoid process inclination, apex expansion and edentulous region anteroposterior elongation with size in non-hadrosaurid hadrosauroids, but a large-scale change in morphology with size in saurolophids. Scaling patterns are significantly different between non-hadrosaurid hadrosauroids and the saurolophid clades along PC1 (Fig. 6C; Table 9). Saurolophine and lambeosaurine patterns are similar to each other (Fig. 6) and cannot be differentiated statistically (Table 9). Along PC2, all high-level clades/grade display significant differences (Table 7; Appendix S5), indicating morphological changes in coronoid process length, dental battery depth and amount of ventralization of the edentulous region with size (non-hadrosaurid hadrosauroids, excluding *E. orientalis*:  $p = 0.006$ , slope =  $0.07279$ ; non-hadrosaurid hadrosauroids, including *E. orientalis*:  $p = 0.008$ , slope =  $0.07252$ ; lambeosaurines:  $p = 0.01$ , slope =  $0.06803$ ; saurolophines, including AMNH 5730:  $p < 0.001$ , slope =  $0.06514$ ;

**TABLE 7.** Simplified statistics from line-fitting analyses: significance (p-value) and degrees of freedom of regression lines in allometry plots (Figs 6C, 7), divided by genus or clade/grade and PC1 or PC2.

Genus/Clade/Grade	Sample size	p-value	F-statistic	Multiple R <sup>2</sup>	Adjusted R <sup>2</sup>	Residual standard error
<b>PC1</b>						
<i>Brachylophosaurus</i>	7	0.162	2.682	0.349	0.219	0.020
<i>Corythosaurus</i>	11	0.128	2.805	0.238	0.153	0.025
<i>Edmontosaurus</i>	7	0.142	3.039	0.378	0.254	0.048
<i>Edmontosaurus</i> excluding AMNH 5730	6	0.150	3.158	0.441	0.302	0.030
<i>Edmontosaurus/Ugrunaaluk</i>	11	< <b>0.001</b>	23.59	0.724	0.693	0.043
<i>Edmontosaurus/Ugrunaaluk</i> excluding AMNH 5730	10	< <b>0.001</b>	29	0.784	0.757	0.0319
<i>Eolambia</i>	4	0.347	1.486	0.426	0.139	0.0149
<i>Gryposaurus</i>	6	0.225	2.05	0.339	0.174	0.019
<i>Prosaurolophus</i>	4	0.105	8.032	0.801	0.701	0.012
Nonhad	19	0.145	2.405	0.156	0.091	0.028
Nonhad including <i>Eotrachodon orientalis</i>	20	0.156	2.247	0.138	0.077	0.028
Lambeosaurinae	32	< <b>0.001</b>	21.48	0.452	0.431	0.026
Saurolophinae	40	< <b>0.001</b>	21.5	0.387	0.369	0.043
Saurolophinae excluding AMNH 5730	39	< <b>0.001</b>	21.64	0.396	0.378	0.036
<b>PC2</b>						
<i>Brachylophosaurus</i>	7	0.269	1.546	0.236	0.084	0.026
<i>Corythosaurus</i>	11	0.308	1.168	0.115	0.017	0.041
<i>Edmontosaurus</i>	7	0.164	2.653	0.347	0.216	0.027
<i>Edmontosaurus</i> excluding AMNH 5730	6	0.272	1.617	0.288	0.110	0.029
<i>Edmontosaurus/Ugrunaaluk</i>	11	< <b>0.001</b>	44.23	0.831	0.812	0.023
<i>Edmontosaurus/Ugrunaaluk</i> excluding AMNH 5730	10	< <b>0.001</b>	35.77	0.817	0.794	0.023
<i>Eolambia</i>	4	0.653	0.274	0.121	-0.319	0.018
<i>Gryposaurus</i>	6	0.423	0.797	0.166	-0.042	0.023
<i>Prosaurolophus</i>	4	0.471	0.778	0.28	-0.080	0.007
Nonhad	19	<b>0.008</b>	9.843	0.431	0.387	0.048
Nonhad including <i>Eotrachodon orientalis</i>	20	<b>0.006</b>	10.53	0.429	0.389	0.046
Lambeosaurinae	32	<b>0.010</b>	7.62	0.227	0.197	0.034
Saurolophinae	40	< <b>0.001</b>	35.74	0.512	0.498	0.027
Saurolophinae excluding AMNH 5730	39	< <b>0.001</b>	32.1	0.493	0.478	0.027

Nonhad, non-hadrosaurid hadrosauroid.

Significant p-values ( $p < 0.05$ ) are in **bold**. All values reported here to three decimal places; detailed statistics can be found in Appendix S5.

saurolophines, excluding AMNH 5730:  $p < 0.001$ , slope = 0.06311). The regression lines of all clades/grade run parallel to each other, differing statistically only in terms of their intercepts, not by their slopes (Fig. 6C; Table 9). In either PC, the exclusion of AMNH 5730 had very little effect on the regression lines (PC1: *Edmontosaurus* with AMNH 5730,  $p = 0.142$ ,  $F = 3.039$ ; *Edmontosaurus* without AMNH 5730,  $p = 0.150$ ,  $F = 3.158$ ; *Edmontosaurus/Ugrunaaluk* with AMNH 5730,  $p < 0.001$ ,  $F = 23.59$ ; *Edmontosaurus/Ugrunaaluk* without AMNH 5730,  $p < 0.001$ ,  $F = 29$ . PC2: *Edmontosaurus* with AMNH 5730,  $p = 0.164$ ,  $F = 2.653$ ; *Edmontosaurus* without AMNH 5730,  $p = 0.272$ ,  $F = 1.617$ ; *Edmontosaurus/Ugrunaaluk* with AMNH 5730,  $p < 0.001$ ,  $F = 44.23$ ; *Edmontosaurus/Ugrunaaluk* without AMNH 5730,  $p < 0.001$ ,

$F = 35.77$ ) (Table 7; Appendix S5). The taxonomic interpretations of *Eotrachodon* as a non-saurolophid hadrosaurid or a non-hadrosaurid hadrosauroid do not matter as the non-hadrosaurid hadrosauroid PC1 regression lines are not significant, and the PC2 regression lines are significant, irrespective of the taxonomic affinity of *Eotrachodon* (Table 7; Appendix S5).

## DISCUSSION

### *The evolution of the hadrosauroid dentary*

Patterns describing the evolution of the hadrosauroid dentary suggest that the coronoid process became taller and

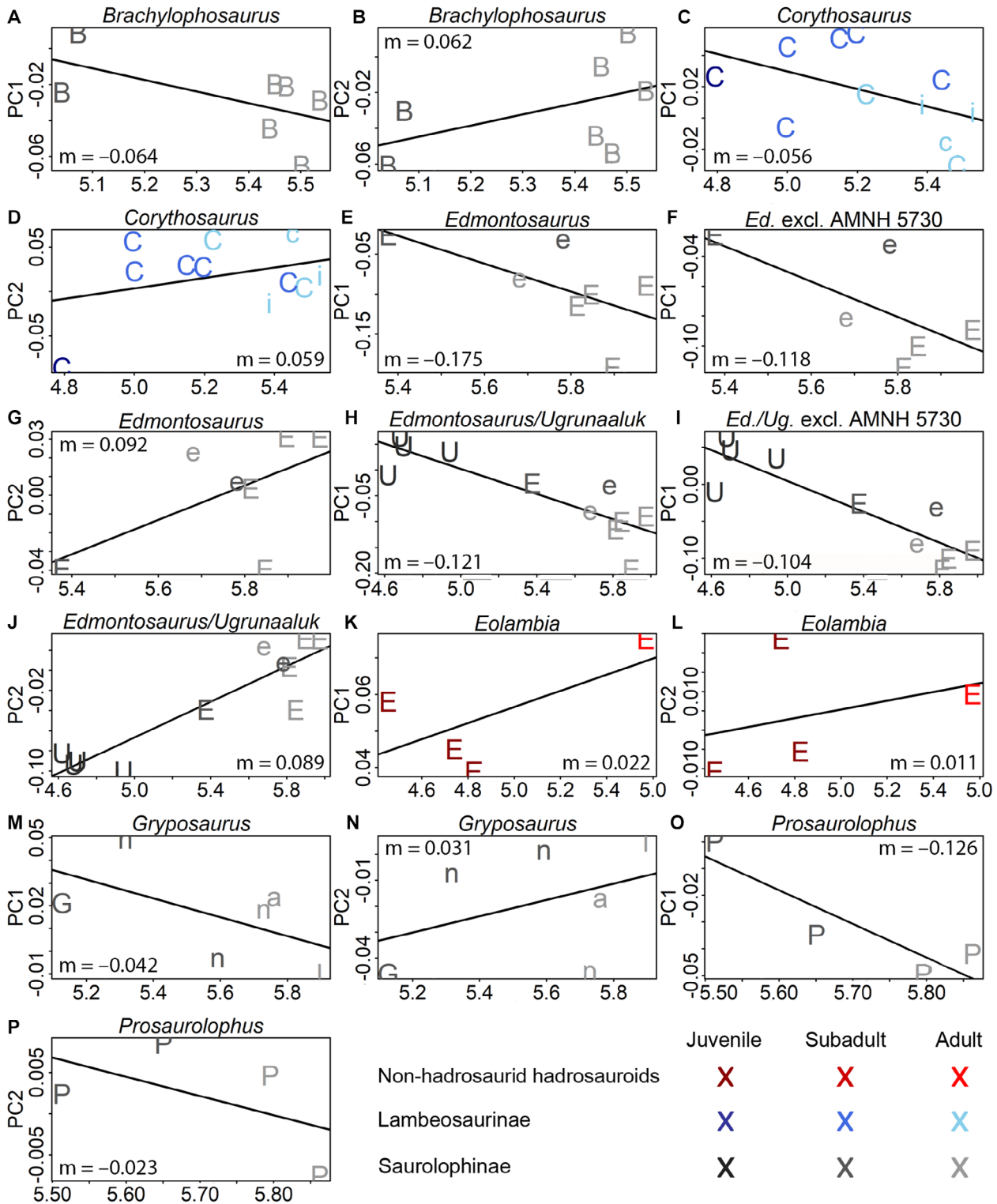


**FIG. 7.** Genus-level allometric scaling. Bivariate plots depict log (natural logarithm) centroid size (x-axis) against PC1 or PC2. The slope coefficient ( $m$ ) is given to three decimal places. Taxonomic and ontogenetic colour scheme as per Figure 5. A–B, *Brachylophosaurus canadensis* (B); C–D, *Corythosaurus casuarius* (c), *C. intermedius* (i) and *Corythosaurus* sp. (C); E and G, *Edmontosaurus annectens* (E) and *E. regalis* (e); F, the *Edmontosaurus* sample, excluding AMNH 5730; H–J, the *Edmontosaurus* sample, including *Ugrunaaluk kuukpikensis* (U); K–L, *Eolambia caroljonesa* (E); M–N, *Gryposaurus alstaei* (a), *G. latidens* (l), *G. notabilis* (n), and *Gryposaurus* sp. (G); and O–P, *Prosaurolophus maximus* (P).



**TABLE 8.** Simplified statistics from standardized major axis (SMA) estimation slope test by genus, including p-values adjusted for multiple comparisons and test statistics.

Genus 1	Genus 2	PC1 p-value	PC1 test statistic	PC2 p-value	PC2 test statistic
<i>Brachylophosaurus</i>	<i>Corythosaurus</i>	1	0.0124	1	0.349
<i>Brachylophosaurus</i>	<i>Edmontosaurus</i>	0.959	2.968	1	0.123
<i>Brachylophosaurus</i>	<i>Edmontosaurus</i> excl. AMNH 5730	1	0.770	1	0.056
<i>Brachylophosaurus</i>	<i>Edmontosaurus</i> = <i>Ugrunaaluk</i>	1	0.408	1	0.391
<i>Brachylophosaurus</i>	<i>Eolambia</i>	0.996	2.182	0.995	2.191
<i>Brachylophosaurus</i>	<i>Gryposaurus</i>	1	0.519	1	0.623
<i>Brachylophosaurus</i>	<i>Prosaurolophus</i>	1	0.248	1	1.608
<i>Brachylophosaurus</i>	<i>Ugrunaaluk</i>	1	0.661	0.993	2.314
<i>Corythosaurus</i>	<i>Edmontosaurus</i>	0.924	3.305	1	0.050
<i>Corythosaurus</i>	<i>Edmontosaurus</i> excl. AMNH 5730	1	0.758	1	0.089
<i>Corythosaurus</i>	<i>Edmontosaurus</i> = <i>Ugrunaaluk</i>	1	0.382	0.982	2.614
<i>Corythosaurus</i>	<i>Eolambia</i>	0.987	2.500	0.933	3.234
<i>Corythosaurus</i>	<i>Gryposaurus</i>	1	0.794	1	1.870
<i>Corythosaurus</i>	<i>Prosaurolophus</i>	1	0.204	0.981	2.635
<i>Corythosaurus</i>	<i>Ugrunaaluk</i>	1	0.625	0.849	3.803
<i>Edmontosaurus</i>	<i>Edmontosaurus</i> excl. AMNH 5730	1	0.720	1	0.008
<i>Edmontosaurus</i>	<i>Edmontosaurus</i> = <i>Ugrunaaluk</i>	0.987	2.503	1	1.269
<i>Edmontosaurus</i>	<i>Eolambia</i>	0.592	5.052	0.974	2.766
<i>Edmontosaurus</i>	<i>Gryposaurus</i>	0.633	4.861	1	1.249
<i>Edmontosaurus</i>	<i>Prosaurolophus</i>	1	1.731	0.996	2.172
<i>Edmontosaurus</i>	<i>Ugrunaaluk</i>	1	0.085	0.931	3.244
<i>Edmontosaurus</i> excl. AMNH 5730	<i>Edmontosaurus</i> = <i>Ugrunaaluk</i>	1	0.252	1	0.755
<i>Edmontosaurus</i> excl. AMNH 5730	<i>Eolambia</i>	0.890	3.554	0.988	2.485
<i>Edmontosaurus</i> excl. AMNH 5730	<i>Gryposaurus</i>	0.996	2.172	1	0.935
<i>Edmontosaurus</i> excl. AMNH 5730	<i>Prosaurolophus</i>	1	0.195	0.999	1.898
<i>Edmontosaurus</i> excl. AMNH 5730	<i>Ugrunaaluk</i>	1	0.064	0.978	2.691
<i>Edmontosaurus</i> = <i>Ugrunaaluk</i>	<i>Eolambia</i>	0.945	3.123	1	1.641
<i>Edmontosaurus</i> = <i>Ugrunaaluk</i>	<i>Gryposaurus</i>	0.998	1.938	1	0.212
<i>Edmontosaurus</i> = <i>Ugrunaaluk</i>	<i>Prosaurolophus</i>	1	0.002	1	1.090
<i>Edmontosaurus</i> = <i>Ugrunaaluk</i>	<i>Ugrunaaluk</i>	1	0.299	1	1.650
<i>Eolambia</i>	<i>Gryposaurus</i>	1	0.952	1	0.876
<i>Eolambia</i>	<i>Prosaurolophus</i>	0.974	2.757	1	0.084
<i>Eolambia</i>	<i>Ugrunaaluk</i>	0.968	2.847	1	0.293
<i>Gryposaurus</i>	<i>Prosaurolophus</i>	1	1.352	1	0.437
<i>Gryposaurus</i>	<i>Ugrunaaluk</i>	1	1.469	1	0.394
<i>Prosaurolophus</i>	<i>Ugrunaaluk</i>	1	0.268	1	0.046

No comparisons were found to be significant. All values reported here to three decimal places; detailed statistics can be found in Appendix S5.

anteriorly inclined with an expanded apex, the edentulous region became more elongate and ventrally deflected, and the dental battery deepened with the addition of more replacement teeth per alveolus. These changes follow

previously observed interspecific dynamics along the hadrosauroid grade leading to Saurolophidae (You *et al.* 2003; Kubota & Kobayashi 2009; Evans 2010; Prieto-Márquez 2010; Norman 2014; Blanco *et al.* 2015). The

**TABLE 9.** Simplified statistics from standardized major axis (SMA) estimation slope and intercept tests by clade/grade, including p-values adjusted for multiple comparisons and test statistics.

Taxonomic affinity 1	Taxonomic affinity 2	PC1 p-value	PC1 test statistic	PC2 p-value	PC2 test statistic
<b>Slope comparison</b>					
Lam	Nonhad	<b>0.011</b>	8.438	0.737	0.841
Lam	Sau	1	0.004	0.102	4.431
Nonhad	Sau	<b>0.008</b>	8.925	0.806	0.646
<b>Intercept comparison</b>					
Lam	Nonhad	0.998	0.027	< <b>0.001</b>	26.670
Lam	Sau	0.836	0.563	< <b>0.001</b>	20.961
Nonhad	Sau	0.916	0.336	< <b>0.001</b>	65.030

Nonhad, non-hadrosaurid hadrosauroid; Lam, lambeosaurine; Sau, saurolophine.

Significant comparisons ( $p < 0.05$ ) in **bold**. All values reported here to three decimal places; detailed statistics can be found in Appendix S5.

dentary of *Eotrachodon* is morphologically similar to that of many non-hadrosaurid hadrosauroids in that it possesses a dorsoventrally short and more dorsally inclined coronoid process with a small apex, an anteroposteriorly short and only slightly ventrally oriented edentulous region, and a dorsoventrally shallow and relatively anteroposteriorly short dental battery when compared to that of many saurolophids (Fig. 5; Tables 3–6). These similarities support a phylogenetic placement outside Hadrosauridae for *Eotrachodon* (*sensu* Xing *et al.* 2017) but also support the hypothesis that major morphological modifications to the hadrosauroid feeding apparatus involving the dentary (and the mandible in general; Stubbs *et al.* 2019) took place at the origin of Saurolophidae.

These morphological transformations led to functional compartmentalization between the acquisition and processing of food items: food acquisition occurred anteriorly (*via* the prementary and premaxillary region of the jaws) and food processing posteriorly, along the dentigerous regions of the maxilla and dentary (Nabavizadeh 2014; Norman 2014). Functional specializations in the masticatory apparatus were probably amplified by ventrally extending rhamphotecae, which were wider and deeper than the premaxilla and prementary bones they ensheathed. This ventral extension of the snout allowed hadrosauroids to crop greater quantities of plant matter at or near ground level while minimizing neck flexion (Farke *et al.* 2013); similar to morphologies observed in some modern low-level grazing bovids (Spencer 1995). Our results support the importance of these previously recognized morphological features, as they represent the main morphological variations described along the first two principal axes of variance (Fig. 5).

Saurolophids occupy regions of the morphospace typified by greater ventral deflection of the edentulous region, consistent with a shift in feeding acquisition strategy from that seen in non-hadrosaurid hadrosauroids (Wyenberg-Henzler *et al.* 2022). The overall lower values along PC2 indicate that adaptations to the consumption of low-growing vegetation were more pronounced in saurolophines than in lambeosaurines (Spencer 1995), the intercept of their regression lines being significantly different (Figs 5, 6C; Table 9). These anatomical differences lend some support to the hypotheses that saurolophines possessed adaptations for living in different habitats than lambeosaurines (e.g. open vs closed habitats), as proposed by Carrano *et al.* (1999), or that they partitioned resources (e.g. Mallon & Anderson 2014). Yet, it also conflicts with other sources suggesting an absence of dietary niche partitioning between lambeosaurines and saurolophines, based on morphometrics (Mallon *et al.* 2013) as well as dental microwear (Wyenberg-Henzler *et al.* 2022). Furthermore, a more ventrally deflected edentulous region in saurolophids than in non-hadrosaurid hadrosauroids suggests improved food processing efficiency, especially in saurolophine saurolophids, associated with improved long-axis rotation of the dentary (Figs 3A–B, 4B; Nabavizadeh & Weishampel 2016).

The anteroposterior motion of the lower jaw (Cuthbertson *et al.* 2012), which worked to move food posteriorly while grinding, was augmented in saurolophids through the development of taller and more anteriorly inclined coronoid processes (Fig. 5; Tables 3, 5) that increased moment arm length. These modifications to the coronoid process redirected the main temporal muscular group, the M. adductor mandibulae externus, that connects the coronoid process to the skull, posteriorly and posterodorsally, increasing mechanical advantage and generating a more effective masticatory system in saurolophids than non-hadrosaurid hadrosauroids (Nabavizadeh 2014, 2016, 2018; Norman 2014; Mallon & Anderson 2015).

The increased depth of the dental battery in saurolophids compared to non-hadrosaurid hadrosauroids of the same ontogenetic stage (Fig. 5, PC2) was probably necessary for the addition of more teeth per tooth family along the hadrosauroid lineage (Norman 2014). Most non-hadrosaurid hadrosauroid taxa have up to three teeth per tooth family (e.g. Head 1998; Kirkland 1998; Norman 1998, 2002; You *et al.* 2003), whereas saurolophid hadrosauroids can have up to seven (Xing *et al.* 2017, *supp. info.*) By increasing the number of teeth in a tooth family, saurolophids integrated a mixture of dead and living structures, thereby adding complexity and improving mastication efficiency (LeBlanc *et al.* 2016). The greater dorsoventral depth of the dental battery in saurolophids may also have been an adaptation for increasing lifelong dentition. An analogous process is seen in modern

hypsodont mammals (e.g. in many artiodactyls and perissodactyls), which have high-crowned, wear-resistant dentitions (i.e. hypsodonty) that maximize the lifetime of a single tooth and hence the lifespan of the individual (Janis & Fortelius 1988; Kilic *et al.* 1997; Fraser & Theodor 2011; Solounias *et al.* 2019). These dentitions are also often accompanied by deeper mandibles and are associated with high-fibre herbivorous diets (e.g. Norman & Weishampel 1985; Janis & Fortelius 1988; Kilic *et al.* 1997; Fraser & Theodor 2011; Solounias *et al.* 2019, especially fig. 1). However, unlike hypsodont mammals, saurolophids achieved a 'high-crowned' structure via stacking teeth.

LeBlanc *et al.* (2016) discovered that, before tooth eruption, the pulp cavity was replaced by dentine, allowing the entire tooth to be obliterated through mastication. Such adaptations benefit from an early onset of development whereby the embryonic and neonatal stages exhibit similar tooth replacement patterns as those found in adults, advancing heterochrony as a mechanism for the early onset of these tissues (LeBlanc *et al.* 2016). Teeth were not a focus of the study here, but the evolution of complex dentitions in saurolophids (Erickson *et al.* 2012) was undoubtedly linked to evolutionary patterns in the dentary. Even though there appear to be taxonomic differences in dental battery depth between these clades/grades, they all show a similar ontogenetic pattern of anteroposterior dental battery elongation during ontogeny (supported by palaeohistological evidence of ontogenetic anteroposterior tooth migration in hadrosaurid dentaries by Bramble *et al.* 2017). As a result, it may be expected that heterochrony and related developmental changes explain the evolution of the saurolophid mandible, as in the case of their teeth and aspects of their postcranial skeleton (e.g. Guenther 2009; LeBlanc *et al.* 2016).

#### *Growth patterns in the hadrosaurid dentary*

Non-hadrosaurid hadrosauroids experienced little or no ontogenetic change in coronoid process inclination, apex size, and relative anteroposterior length of the edentulous region (PC1, Table 4). Most changes in this group occurred along PC2 (compare Fig. 8C with F), associated with decreased ventralization of the edentulous region, anteroposterior elongation of the dental battery (and the dentary overall) leading to a shorter coronoid process relative to the anteroposterior length of the dentary (Figs 5, 6). These ontogenetic changes were likely to have been gradual, given that juveniles and adults differ significantly, but neither differs from subadults (Table 6). However, intraspecific sampling of non-hadrosaurid hadrosaurid taxa is limited, and many are represented by a single growth stage. Only *Bactrosaurus johnsoni* and *Eolambia*

*caroljonesa* are represented by specimens at both juvenile and adult stages. As a result, we cannot unambiguously reject that differences represent a taxonomic rather than ontogenetic signal.

None of the lambeosaurine ontogenetic stages differ significantly from each other. Juvenile lambeosaurines, however, occupy a morphospace range that is quite narrow and the sample is small ( $N = 3$ ). Given the small sample, more extreme morphologies, positioned outside this range, might have been excluded, potentially altering the outcome of the statistical tests, especially as a significant difference is found when lambeosaurines are compared to both non-hadrosaurid hadrosauroids and saurolophines as a whole (Table 3), and visually, lambeosaurine adults appear morphologically intermediate between non-hadrosaurid hadrosaurid and saurolophine adults (Figs 5, 8C).

In saurolophines, the increase in coronoid process inclination, apex expansion, and relative length of the edentulous region (Figs 5, 6A, PC1) is also reflected in the statistical tests (Table 4), where juveniles are significantly different from adults; however, subadults cannot be distinguished from juveniles, nor adults. These patterns indicate gradual ontogenetic changes in these structures (Fig 8B, C). A shift in coronoid process morphology was observed in the growth of *Edmontosaurus annectens*, with considerable variation in angle among juveniles (*c.* 71–80° from the horizontal axis; Wosik *et al.* 2019; Takasaki *et al.* 2020). A gradual, growth-related increase in the edentulous region is also generally recovered in *Edmontosaurus* (Campione & Evans 2011; Wosik *et al.* 2019; Takasaki *et al.* 2020). The edentulous region of hadrosauroids is analogous to the diastema observed in many herbivorous mammals that, in several North American artiodactyls (e.g. *Antilocapra americana*, *Cervus canadensis*, *Odocoileus virginianus* and *Ovis canadensis*), undergoes ontogenetic anteroposterior elongation (Moyano *et al.* 2020). The presence of these dental gaps supports current hypotheses on the convergent food-collection anatomy between evolutionarily distant groups such as hadrosauroids and extant mammals (e.g. Carrano *et al.* 1999; Nabavizadeh 2018). However, our results reveal that these ecological adaptations are also associated with convergent developmental changes.

Ontogenetic changes in dentary morphology are present in both non-hadrosaurid hadrosauroids, lambeosaurines and saurolophines, and along PC2 include decreased ventralization (de-ventralization) of the edentulous region, as well as anteroposterior elongation of the dental battery (and hence that of the dentary) causing the height of the coronoid process compared to that of the length of the dentary to be shorter in relative dimensions (Figs 5, 6, 8E–F). These ontogenetic changes were likely to have been gradual, as seen by the significant difference in

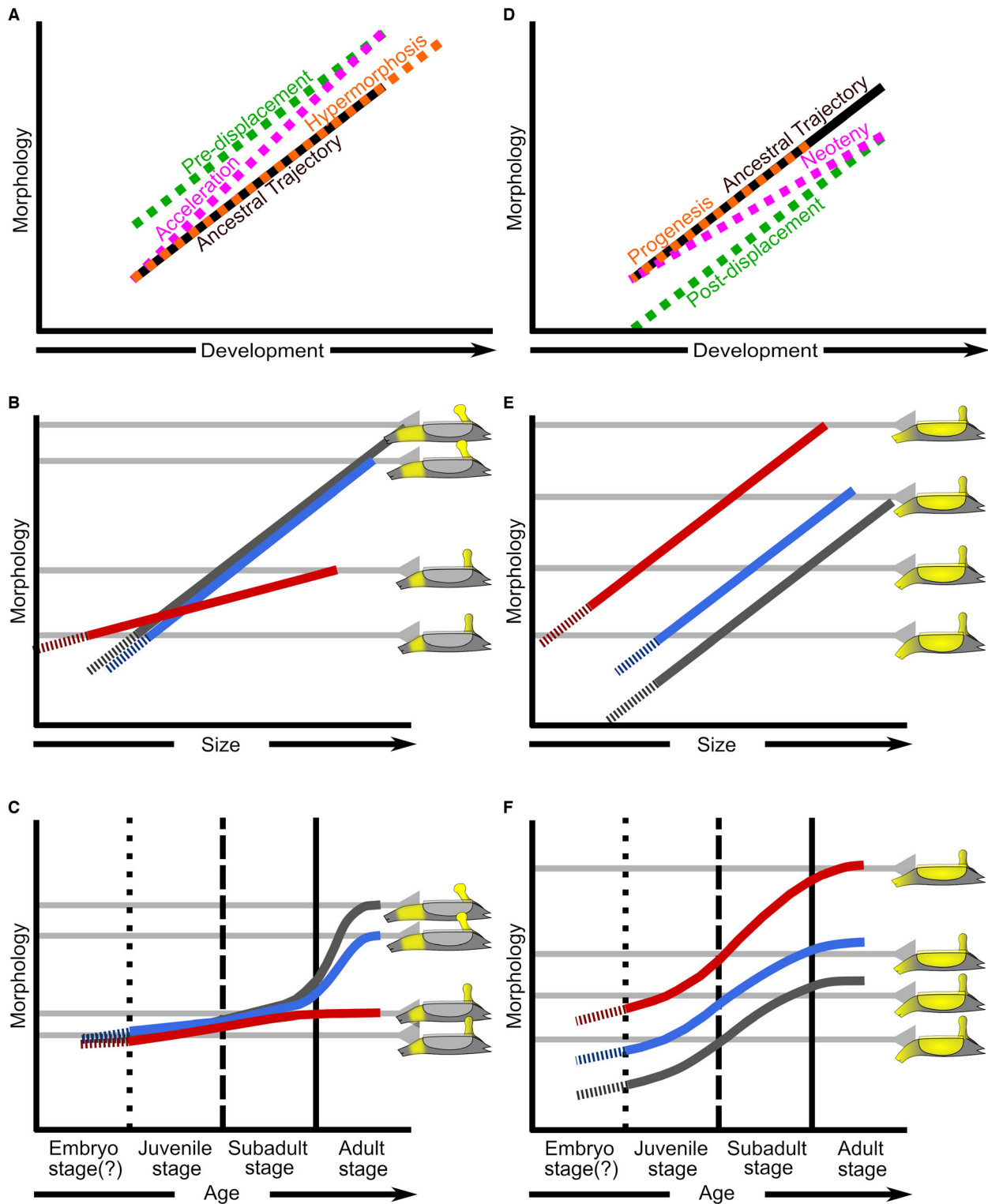


**FIG. 8.** Conceptual diagrams summarizing heterochronic processes and their developmental predications. Peramorphic (A) and pae-  
domorphic (D) processes relative to an ancestral trajectory, modified from figures and concepts presented by Alberch *et al.* (1979).  
B, E, stylized versions of the results presented in this study; colours as per Figure 5, broken lines represent the inferred embryonic  
stage, and the approximate morphological changes in dentary traits are highlighted in yellow on dentary drawings adjacent to dia-  
grams. C, F, developmental models of: C, hypermorphic/accelerated dentary traits along PC1; F, post-displaced dentary traits along  
PC2.

morphology between juveniles and adults, but not between juveniles and subadults, nor between subadults and adults for each of the separate grade/clades (Table 6). De-ventralization of the edentulous region during ontogeny could be interpreted as a possible ontogenetic change in diet or an increase in the dentary's ability to rotate along its anteroposterior axis leading to improved mastication biomechanics (Spencer 1995; Nabavizadeh & Weishampel 2016). Anteroposterior elongation of the dental battery relates to an ontogenetic increase in the number of alveoli, as previously reported (Bramble *et al.* 2017; Wosik *et al.* 2019), serving to increase the available occlusion surface area for processing food. A convergent dental pattern is again seen in herbivorous mammals (e.g. *Antilocapra americana*), where growth-related increases in the occlusal area are associated with increased food processing abilities needed to sustain a larger individual (Moyano *et al.* 2020). It is likely that an increase in food processing ability was needed in hadrosauroids given that they grew by three orders of magnitude during ontogeny (Wosik *et al.* 2020).

#### *A developmental model for the evolution of the hadrosauroid feeding apparatus*

Our results reveal significant developmental changes in the hadrosauroid dentary from juvenile to adult stages. Many of these changes parallel the macroevolutionary dynamics that led to the morphologies observed in the saurolophid dentary. Accordingly, we propose that the evolutionary history of the saurolophid dentary is best described by a combination of heterochronic events. Heterochrony is an evolutionary pattern in which the timing (onset), rate, or duration of a developmental event is altered in one species from that seen in its ancestor (Smith 2001; McNamara 2012; Schoch 2014). There are many types of heterochronic shift, but these are typically dichotomized into peramorphosis and paedomorphosis. Peramorphosis is the increase of development, whereby the ontogenetic trajectory of the descendant species extends beyond that of the ancestor (Fig. 8A). The opposite, paedomorphosis, is the decrease of development, which generally manifests as the retention of an ancestral juvenile feature in the adults of a descendant species (Fig. 8D; McNamara 2012; Schoch 2014). In the evolutionary history of the hadrosauroid dentary, we hypothesize that: (1) *peramorphosis* can explain the relative anteroposterior elongation of the edentulous region, anterior inclination and apex expansion of the coronoid process (Figs 5, 6C (PC1), 8B–C); and (2) the relative dorsoventral length of the coronoid process, dorsoventral depth of the dental battery, and ventral deflection of the

edentulous region all represent *paedomorphic* changes (Figs 5, 6C (PC2), 8E–F).

*Peramorphosis*. There are three different peramorphic types: (1) acceleration, whereby development is sped up but starts and ends at the same age; (2) hypermorphosis, whereby the developmental trajectory is extended due to later termination of development; and (3) pre-displacement, whereby the onset of the developmental event takes place earlier in ontogeny, but rate and age-at-maturity are the same (Fig. 8A; Alberch *et al.* 1979; McNamara 2012; Schoch 2014). Importantly, pre-displacement predicts differential morphologies across all ontogenetic stages (Fig. 8A). The angle of the coronoid process, expansion of its apex and the relative length of the edentulous region in saurolophid juveniles and subadults are not significantly different from that of non-hadrosauroid hadrosauroid juveniles and subadults (Table 4), rejecting the predictions of pre-displacement. Acceleration predicts a divergent trajectory, whereby juveniles are indistinguishable, but trajectories become increasingly more differentiated throughout ontogeny. Although we did not recover significant differences between subadult stages, linear models along PC1 appear to diverge as a function of size (Fig. 6C), overall consistent with acceleration. Finally, the existence of a significant difference between non-hadrosauroid hadrosauroid adults and saurolophid adults (Fig. 5; Table 4) suggests that most differentiation takes place after reaching the age of maturity, during the saurolophid adult stage. Accordingly, the patterns obtained herein indicate an extension, and possible speeding-up, of the developmental trajectory among saurolophids, consistent with hypermorphosis and/or acceleration in the relative length of the edentulous region, the anterior inclination of the coronoid process and expansion of its apex (Fig. 8A–C). Given the dietary role played by the aforementioned structures, we propose that these heterochronic shifts were associated with increased feeding efficiency, which may support the hypothesis that saurolophids underwent shifts in diet as they grew (Wyenbergh-Henzler 2022; Wyenbergh-Henzler *et al.* 2022) or, at the very least, expanded their feeding envelope (Mallon *et al.* 2013).

Peramorphosis in saurolophids is not unique to the dentary. For instance, palaeohistological analyses show that by infilling the root with dentine, saurolophids could retain older tooth generations, incorporating them into the grinding surface (LeBlanc *et al.* 2016). Lambeosaurines are thought to have experienced pre-displacement of the cranial crest, and the crest of *Parasaurolophus* may have undergone both pre-displacement and hypermorphosis relative to other lambeosaurines (Farke *et al.* 2013). Post-cranially, the lambeosaurine *Hypacrosaurus* shows pre-displacement in the development of the supraacetabular

process of the ilium, with an earlier onset compared to saurolophines such as *Brachylophosaurus* and *Maiasaura*, and non-hadrosaurid hadrosauroids (Guenther 2009). Together, these studies and ours support the idea that major components of the saurolophid Bauplan can be attributed to heterochronic shifts across the non-hadrosaurid hadrosauroid to saurolophid transition.

*Paedomorphosis.* Paedomorphosis is also categorized into three distinct sub-processes: (1) neoteny, whereby the rate of development is slowed down compared to that of the ancestor but starts and ends at the same age; (2) progenesis, whereby the descendant's developmental trajectory ends earlier in ontogeny than the ancestor due to the earlier onset of maturation; or (3) post-displacement, whereby the onset of development in the descendant is delayed, but the rate and age-at-maturity remain constant (Fig. 8D; Alberch *et al.* 1979; Schoch 2014).

Neoteny predicts a change in the rate of development, which is inconsistent with the similar allometric trajectories between non-hadrosaurid hadrosauroids and the saurolophids along PC2 (Fig. 6C). Progenesis can also be rejected as it predicts that juveniles and subadults will be morphologically similar, which is not the case here (Fig. 5; Table 6). Furthermore, the morphospace range of all taxonomic groups is subequal along PC2 (Figs 5, 6C), contrasting the decreased morphological variability predicted by a progenitally truncated developmental trajectory. By contrast, post-displacement is supported, stipulating a delay in the edentulous region de-ventralization and anteroposterior dental battery elongation. This delay leads to dentaries that appear anteroposteriorly shorter but dorsoventrally taller in saurolophids than those of non-hadrosaurid hadrosauroids (Fig. 8D–F). This process may have prevented saurolophid adults from reaching the same morphology as non-hadrosaurid hadrosauroid adults, causing the entire growth trajectory of saurolophids to shift negatively along PC2 (Figs 5, 6C, 8D–F; Table 9).

Theoretical depictions of post-displacement are typically bivariate, relating shape against age (developmental time since birth; e.g. Alberch *et al.* 1979, fig. 20A; Fig. 8D). By contrast, our results depict shape versus size. Birth or hatching will always occur at age zero, but not necessarily at the same size (compare Fig. 8E with F). Therefore, although our preferred interpretation for PC2 is post-displacement, interspecific size differences resulting from macroevolutionary shifts could also explain the recovered shifts (Fig. 6C). Furthermore, morphology can change at variable rates during different ontogenetic stages (e.g. Figs 6C, 8F), which, if compared to a size standard (rather than age) may appear more linear.

Saurolophid juveniles display a condition in the traits related to the orientation of the edentulous region, height

of the coronoid process, and depth of the dental battery, unlike any non-hadrosaurid hadrosauroid growth stage analysed herein. It is possible that if the allometric trajectory of non-hadrosaurid hadrosauroids was extrapolated to the embryonic stage, they would exhibit a similar morphology to that of saurolophid juveniles (Fig. 8E, F). However, a sample of non-hadrosaurid embryonic specimens would be needed to explore this possibility. This post-displacement shift along the shape axis (PC2) also explains why saurolophids do not reach the juvenile non-hadrosaurid hadrosauroid morphology until subadulthood or adulthood, as the onset of growth is delayed, but the termination of growth stays the same, resulting in a shorter growth trajectory that starts and ends with a shape seemingly more immature than the ancestor (Figs 5, 6C, 8E–F; Table 6).

Through post-displacement, the dentary became anteroposteriorly shorter but dorsoventrally deeper in saurolophids, compared to that of those of non-hadrosaurid hadrosauroids (Figs 5, 6C, 8E–F). Deepening of the battery corresponds to an increase in the number of vertically stacked teeth per tooth family in saurolophids (e.g. maximum of seven teeth per alveolus in the dentary of *Edmontosaurus regalis*, Xing *et al.* 2017, supp. info.) contrasted with that of non-hadrosaurid hadrosauroids (a maximum of three dentary teeth per alveolus; Head 1998; Kirkland 1998; Norman 1998, 2002; You *et al.* 2003). Furthermore, the generation of more teeth has previously been linked to the accelerated deposition of orthodontine and cementum during dental development in embryonic and neonatal saurolophids (LeBlanc *et al.* 2016).

Overall, the heterochronic changes in the hadrosauroid dentary support the hypothesis that food selection was associated with processing adaptations that increased the rate of food intake/digestion, thus sustaining the evolution of larger body sizes in saurolophids (Benson *et al.* 2014, 2018). The three groups of hadrosauroids discussed in this study experienced ontogenetic anteroposterior elongation of the dental battery, increasing the number of alveoli and leading to larger surface areas to grind plant matter. Combined with increases in the relative length of the edentulous region, saurolophids developed elongated jaws. These transformations increased mechanical advantage, directed muscles to pull posteriorly, and allowed functional specialization of the predentary and dental batteries through their increased separation (Nabavizadeh 2014, 2016; Norman 2014).

#### *Comments on the edmontosaurin from the Prince Creek Formation of Alaska*

The specimens of *Ugrunaaluk kuukpikensis* included in the present analysis are from the Liscomb bonebed of the

Prince Creek Formation in northern Alaska (Mori *et al.* 2016), but were previously referred to *Edmontosaurus* sp. (Gangloff & Fiorillo 2010). Using a dataset of linear measurements, Mori *et al.* (2016) erected *Ugrunaaluk kuukpikensis* based on a unique combination of characters. Notably, the Prince Creek Formation material is comprised solely of immature specimens, which is likely to affect phylogenetic placement (Tsuihiji *et al.* 2011; Campione *et al.* 2013; Prieto-Márquez 2014; Poole 2022). Combined with the significant morphological divergence between both known *Edmontosaurus* species (see Campione & Evans 2011), subsequent studies have favoured the more conservative return to *Edmontosaurus* sp. (Xing *et al.* 2017; Wosik *et al.* 2019; Takasaki *et al.* 2020).

To compare the morphology of the Prince Creek Formation dentaries to *Edmontosaurus annectens* and *E. regalis*, the dentaries of these taxa were pooled into bivariate allometry plots. Comparing the combined Prince Creek Formation dentaries and *Edmontosaurus* spp. regression lines with that of only *Edmontosaurus* (Fig. 7E–J) shows that the two taxa are not significantly different (PC1  $p = 0.987$ ; PC2  $p = 1$ ; Table 8). Dentary isometry can be rejected in favour of allometry only by the increase of specimens and size range that comes from pooling the Prince Creek Formation dentaries and *Edmontosaurus* dentaries into the same regression (PC1  $p < 0.001$ , PC2  $p < 0.001$ ; Table 7). This could either indicate support for *U. kuukpikensis* as being separate from *Edmontosaurus*, or support referral of the Prince Creek Formation material to *Edmontosaurus*, in which case the dentary of *Edmontosaurus* spp. would show an allometric increase in the length and inclination of the coronoid process, size of its apex, relative anteroposterior dental battery as well as edentulous region length and de-ventralization during development. A previous study stated that one out of the

three characteristics used to separate *Edmontosaurus* from the Prince Creek Formation specimens, namely a short symphyseal process, showed significant amounts of ontogenetic plasticity in its morphology, and based on its ratio with total dentary length, they also found it impossible to distinguish this in the Prince Creek Formation specimens from the slightly larger juvenile *E. annectens* specimens from the Hell Creek Formation (Wosik *et al.* 2019). Furthermore, three of the six synapomorphies tying these specimens and *Edmontosaurus* together into one clade are ontogenetically variable, two of which pertain to the dentary: the coronoid process being moderately angled anteriorly, and the slope of the edentulous region being rather short (Takasaki *et al.* 2020). As long as the Prince Creek Formation specimens belong to *Edmontosaurus* sp., this aforementioned ontogenetic variability (Wosik *et al.* 2019; Takasaki *et al.* 2020) is supported herein (Fig. 5, Fig. S2; Table 8). Ultimately, we agree that juvenile *Edmontosaurus* specimens contemporary to the Prince Creek Formation specimens but from lower latitudes, or adult *Ugrunaaluk* specimens should be obtained to properly assess the connection between *Edmontosaurus*, *Ugrunaaluk*, their ontogenetic changes and taxonomic validity (Xing *et al.* 2017; Wosik *et al.* 2019; Takasaki *et al.* 2020).

#### Implications for phylogenetically informative characters of the dentary

The dentary is an important source of phylogenetic information, representing approximately 8.5–16% of the characters in character–taxon matrices over the last few decades (Table 10). The fundamental assumption of all phylogenetic characters is that they represent taxonomic

**TABLE 10.** Numbers of dentary-related characters in the literature.

Source*	Dentary teeth	Dentary bone	Dentary teeth + bone	Number of characters
Weishampel <i>et al.</i> 1993	4 (10.8%)	2 (5.4%)	6 (16.2%)	37
Godefroit <i>et al.</i> 2008	3 (5.4%)	2 (3.6%)	5 (8.9%)	56
Evans & Reisz 2007; Evans 2010	5 (5.3%)	4 (4.3%)	9 (9.6%)	94
Prieto-Márquez 2010	14 (3.8%)	21 (5.7%)	35 (9.5%)	370
Xing <i>et al.</i> 2014	15 (4.3%)	21 (6.1%)	36 (10.4%)	345
Prieto-Márquez <i>et al.</i> 2016	10 (3.7%)	14 (5.1%)	24 (8.8%)	273
Xing <i>et al.</i> 2017	17 (4.9%)	22 (6.4%)	39 (11.3%)	346
Prieto-Márquez <i>et al.</i> 2019	10 (3.6%)	14 (5%)	24 (8.6%)	280
Gates <i>et al.</i> 2021	10 (3.5%)	14 (4.9%)	24 (8.4%)	286
McDonald <i>et al.</i> 2021	5 (2.5%)	12 (5.9%)	17 (8.4%)	203
Prieto-Márquez & Carrera Farias 2021	11 (3.9%)	15 (5.3%)	26 (9.2%)	283

Percentage (in parentheses) is relative to the total number of characters in that publication's character–taxon matrix.

\*See supporting information files for each reference.

and phylogenetic variation at a level commensurate with the operational taxonomic units (e.g. genus or species). However, relatively few phylogenetic studies explicitly consider the range of intra- versus intertaxonomic variation, when constructing characters (but see Prieto-Márquez 2010). As a result, the results presented here have important implications for the definition of dentary phylogenetic characters of hadrosauroid ornithopods. As there are many phylogenetic matrices (see Table 10), the following discussion focuses on two extensive datasets, those of Xing *et al.* (2017) and Prieto-Márquez & Carrera Farias (2021), and explores characters associated with the edentulous region, the coronoid process, and the dental battery.

*The edentulous region.* This part of the dentary is typically represented by three characters, the first being the ratio of the edentulous region's length relative to the distance from the anteriormost alveolus to the posterior margin of the coronoid process (Xing *et al.* 2017, char. 38, [0] = <0.20, [1] = 0.20–0.31, [2] > 0.31–0.45, [3] > 0.45; Prieto-Márquez & Carrera Farias 2021, char. 26, [0] < 0.20, with a sample mean of 0.11, [1] = 0.20–0.31, with a sample mean of 0.27, [2] = 0.32–0.45, with a sample mean of 0.35, [3] > 0.45, with a sample mean of 0.54), which is also a synapomorphy of the genus *Edmontosaurus* (Xing *et al.* 2017, char. 38 [3]). The relative length of the edentulous region varies along PC1, separating adult non-hadrosauroid hadrosauroids from saurolophids, and even separating lambeosaurines and saurolophines if *Eotrachodon* is considered a non-hadrosauroid hadrosauroid (Figs 5, 6; Tables 3, 9). However, the relative length of the edentulous region also varies ontogenetically, with sometimes large variation present among juvenile saurolophid specimens, that also resemble the primitive condition seen in non-saurolophid hadrosauroids (Figs 5–7; Table 4). Of note, variation between non-hadrosauroid hadrosauroid growth stages appears independent of growth stage, supporting indiscriminate use of the aforementioned characters to code non-hadrosauroid hadrosauroids. However, only adult saurolophid specimens should be used to code characters pertaining to the length of the edentulous region of the dentary.

The second and third phylogenetic characters relate to the shape of the dorsal margin of the edentulous region (Xing *et al.* 2017, char. 45, [0] = a gradually descending and smooth dorsal margin in the dentary's anterodorsal region, [1] = a dorsal margin that is quite steep, forming a prominent depression in the symphyseal region of the dentary; Prieto-Márquez & Carrera Farias 2021, char. 29, [0] = displaying a very slight concavity, to being straight, to slight convexity, [1] = displaying a very clear concavity) and the ventral deflection of the edentulous region of

the dentary (Xing *et al.* 2017, char. 41, [0] = faintly ventrally deflected, angle <17°, [1] = moderately ventrally deflected, angle between 17 and 25°, [2] deflected ventrally to a marked degree, angle >25°; Prieto-Márquez & Carrera Farias 2021, char. 27, [0] <17°, with a sample mean of 13°, [1] 17–25°, with a sample mean of 22°, [2] >25°, with a sample mean of 33°). Both the ventral deflection and the shape of the edentulous region vary along PC2 (Fig. 5), and are weakly pronounced at the positive end. Significant separation is seen between all different taxonomic groups, indicating the suitability of these characters to distinguish between non-hadrosauroid hadrosauroids and saurolophids (Figs 5, 6; Tables 5, 6, 9). Lambeosaurines show significant differences from saurolophines as a whole (Tables 5, 9), but not when only adults are considered (Table 6), questioning the overall utility of these characters to separate the two saurolophid clades. Both of these characters are ontogenetically variable in all taxonomic groups as juveniles and adults show significant differences (Figs 5, 6; Table 6). Therefore, immature saurolophid specimens are unsuitable for coding these characters. While other research has stated that the non-hadrosauroid hadrosauroid *Eolambia* shows less of a ventral angle of the edentulous region in larger than smaller specimens (Poole 2022), suggesting ontogenetic variability, this pattern was not recovered for *Eolambia* adults and juveniles herein (Fig. 5). Additionally, some taxa show high individual variation at certain growth stages (e.g. *Edmontosaurus*, *Brachylophosaurus*, *Corythosaurus* and specimens previously attributed to the now *nomen vanum* *Willinakaqe* (Cruzado-Caballero & Coria 2016); Fig. 5).

*The coronoid process.* The orientation of the coronoid process is a character commonly present in hadrosauroid character–taxon matrices (e.g. Xing *et al.* 2017, char. 48, orientation of the coronoid process relative to the dorsal margin of the dentary, [0] = vertical or posteriorly inclined, [1] = inclined slightly anteriorly, angle 70–85°, [2] = inclination obviously anterior, angle <70°; Prieto-Márquez & Carrera Farias 2021, char. 30, orientation of the coronoid process relative to the alveolar margin of the dental battery, [0] ≥ 80°, [1] < 80°) and is also a synapomorphy of *Edmontosaurus* (Xing *et al.* 2017, char. 48 [2]). Coronoid process inclination varies along PC1, indicating its variability in hadrosauroids and supporting its taxonomic utility to separate non-hadrosauroid hadrosauroids and saurolophids (Figs 5, 6; Tables 3, 9). Most saurolophids show qualitatively that morphologies that are ontogenetically variable (Figs 5, 6), with quantitative results supporting this assessment for most saurolophines (juveniles with more vertical coronoid process, significantly different from adults with a much more anteriorly



angled coronoid process), and for lambeosaurines if *Eotrachodon* is considered a non-hadrosaurid hadrosaurid (and then juveniles are significantly different from adults) (Table 4). Examples of this include *Ugrunaaluk* if it is considered to be *Edmontosaurus* sp. (similarly observed in the transition from subadult to adult stage in *Edmontosaurus annectens* by Wosik *et al.* 2019), as well as *Corythosaurus* from subadult to adult stages (Figs 5, 7C, H–I). When saurolophid individual variation in inclination of the coronoid process is examined, it is evident that saurolophids display a substantial variation (Fig. 5; e.g. juvenile specimens of *Ugrunaaluk*, specimens of *nomen vanum Willinakaqe*; adult specimens of *Brachylophosaurus canadensis*, *Edmontosaurus*, *Corythosaurus*, *Lambeosaurus lambei* and *Tsintaosaurus spinorhinus*). The wide individual and ontogenetic variation in some of these genera probably extends into more than one state of character 48 of Xing *et al.* (2017), and possibly that of Prieto-Márquez & Carrera Farias (2021) as well. However, the states described for character 30 of Prieto-Márquez & Carrera Farias (2021) are likely to be more suitable for the taxonomic variation seen in the inclination of the coronoid process, providing a more clear separation between non-hadrosaurid hadrosauroids and saurolophids than those in Xing *et al.* (2017)'s character 48. Therefore, we recommend that specimens of all non-hadrosaurid hadrosaurid growth stages, but only adult specimens in saurolophids, be used when coding the aforementioned characters, and that the range of individual variation in hadrosaurid dentary morphology be further investigated through linear measurements.

In our exploration of dentary variance, we found notable taxonomic variation in the relative height of the coronoid process, a variation that is explicitly missing from character–taxon matrices of Prieto-Márquez & Carrera Farias (2021) and Xing *et al.* (2017). Previous research has shown that the coronoid process became taller in saurolophines than in non-hadrosaurid hadrosauroids (Norman 2014). However, relative coronoid process height is also ontogenetically variable in non-hadrosaurid hadrosauroids (with the possible exceptions of the non-hadrosaurid hadrosauroids *B. johnsoni* and *E. caroljonesa*; Figs 5, 7L), and many saurolophid taxa specifically from subadult to adult stage (with the possible exception of *Gryposaurus*; Fig. 7N) and in some instances from juvenile to older ontogenetic stages (e.g. *Ugrunaaluk* if synonymized with *Edmontosaurus* sp., and *Corythosaurus*; Figs 5, 7D, J). Thus, we recommend that future phylogenetic matrices include a ratio describing the variation in the relative height of the coronoid process, as this is likely to provide good separation of non-hadrosaurid hadrosauroids from saurolophids, and lambeosaurines from saurolophines (Table 5). This could take the form of a ratio between the height of the coronoid process (measured from the mid-

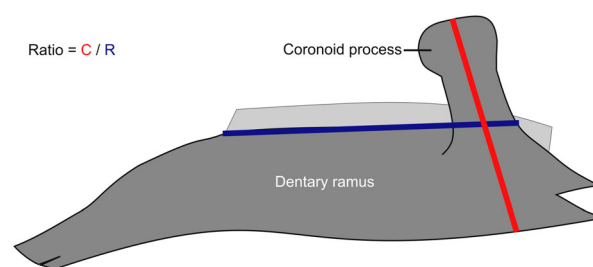


**FIG. 9.** Schematic drawing of a hadrosaurid dentary in lateral view with the coronoid process height ratio proposed herein. The red line is the coronoid process length (C), measured from the dorsalmost point mid-way between the anterior and posterior edges of the coronoid process apex, parallel to the long axis of the process, to the ventral margin of the dentary. The blue line is the reference line (R), measured from the anteriormost tooth, along the ramus' dorsal edge, to the posterior margin of the coronoid process.

width of the dorsal margin of its apex to the ventral margin of the dentary) and the length of the dental battery (measured along the ramus' dorsal edge from the anterior-most tooth position to the posterior margin of the coronoid process) (Fig. 9). Testing the validity of the suggested ratio would best be done on a separate dataset of linear measurements on hadrosaurid dentaries, as it could include additional specimens not included here due to incompleteness (e.g. specimens including the coronoid process and dental battery but missing the edentulous region, which had to be excluded herein), thereby increasing sample size. Much like other characters explored here, we recommend that this ratio be measured only in adults for most taxa as juveniles are likely to exhibit the primitive condition.

*The dental battery.* A character typically present in character–taxon matrices is one that reflects the maximum number of tooth positions (alveoli) in the dentary dental battery (Xing *et al.* 2017, char. 1, [0] ≤ 30, [1] = 31–45, [2] > 45; Prieto-Márquez & Carrera Farias 2021, char. 1, [0] ≤ 30, with a sample mean of 22, [1] = 31–42, with a sample mean of 37, [2] > 42, with a sample mean of 49), a synapomorphy which supports *Shantungosaurus* as the sister of *Edmontosaurus* (Xing *et al.* 2017, char. 1[2]). During ontogeny, all taxonomic groups display gradual antero-posterior elongation of dental batteries (Figs 5, 6; Table 6), and hence a greater number of tooth families. The number of tooth families in *Eolambia caroljonesa* and *Bactrosaurus johnsoni* is growth independent (alveolar positions <30) (Weishampel 1984; Kirkland 1998; You *et al.* 2003), representing the plesiomorphic condition (i.e. char. 1 [0] in both Xing *et al.* 2017 and Prieto-Márquez & Carrera Farias 2021) for Hadrosauroida. These species illustrate a situation that may occur in other hadrosaurid outgroups, allowing the number of alveolar positions to possibly still

(cautiously) be scored regardless of the amount of ontogenetic development. However, within Lambeosaurinae, the ontogenetic increase in tooth families spans more than one character state, for example, *Hypacrosaurus stebingeri* (embryos MOR 559 with 8 and RTMP 89.79.52 with 8 or 9 tooth positions, the nestling MOR 548 with 20 (Horner & Currie 1994); subadult TMP 1994.385.01 with 30 (Brink *et al.* 2011); adult MOR 549 with 41 (Prieto-Márquez 2008, p. 263)) and *Corythosaurus casuarius* (juvenile ROM 759 with approximately 20 tooth families (Evans 2007, p. 112); adults ROM 1933 and ROM 868 with 37 and 38 (Prieto-Márquez 2008, p. 263)). The same is true for Saurolophinae, for example, in *Gryposaurus notabilis* (juvenile ROM 1939 with 25 tooth families (Mallon *et al.* 2022); large individuals with up to 40 (Lull & Wright 1942)) and *Edmontosaurus annectens* (juvenile UCMP 235860 with 9 tooth families, and subadult ROM 73859 with 44 (Wosik *et al.* 2019); adult specimens with up to 55 (Prieto-Márquez 2008, p. 263)). This ontogenetic variation in relative anteroposterior dental battery length indicates that only adults should be used to score the number of alveolar positions in Saurolophidae.

## LIMITATIONS AND CONCLUSION

Results support several previously reported evolutionary trends in the hadrosauroid dentary, as well as a highly intertwined pattern of growth-related evolutionary changes in this element during the transition from non-hadrosaurid hadrosauroids to saurolophids. These heterochronic transformations were likely to have enhanced food gathering and food processing abilities, accommodating the increased energy demands of larger-bodied saurolophids (Benson *et al.* 2014, 2018).

Hypermorphosis and/or acceleration, peramorphic processes resulting in an extension or acceleration, respectively, of the development in descendant taxa relative to that of ancestral species (Alberch *et al.* 1979; Schoch 2014), are hypothesized for the changes relating to the relative anteroposterior elongation of the edentulous region and increased anterior inclination of the coronoid process as well as expansion of its apex in saurolophids. This separation permitted food-gathering and processing specialization of the prementary and dental battery (Norman 2014), and increased mechanical advantage, which led to increased masticatory efficiency and increased the available area for muscle attachment (Nabavizadeh 2014, 2018; Norman 2014), respectively.

Post-displacement, a pedomorphic process resulting in the delay of onset of development and hence an adult morphology in the descendant taxa reminiscent of an immature ancestor (Alberch *et al.* 1979; Schoch 2014), is hypothesized for the changes relating to the relative

dorsoventral height of the coronoid process, the relative dorsoventral depth of the dental battery, and the increased ventral orientation of the edentulous region in saurolophids. This increased moment arm length and redirected muscles to pull the jaw more posteriorly (Norman 2014; Nabavizadeh 2016, 2018), increased the number of tooth rows (Head 1998; Kirkland 1998; Norman 1998, 2002; You *et al.* 2003; Xing *et al.* 2017, supp. info.) that both worked as masticatory shock-absorbers and allowed teeth to be replaced continuously as the functional row was worn down (LeBlanc *et al.* 2016), and increased long-axis dentary rotation involved in improved mastication biomechanics (Nabavizadeh & Weishampel 2016) as well as possibly served as an adaptation to low-growing vegetation (Spencer 1995), respectively.

During growth, both non-hadrosaurid hadrosauroids and saurolophids experienced anteroposterior elongation of the dental battery, incorporating more teeth per row, as well as a decrease in the heterochronically-induced ventral orientation of the edentulous region. Overall, the combination of these evolutionary and growth-related modifications to the dentary is likely to have helped saurolophids become very abundant and reach a near-global distribution in the Late Cretaceous.

One limitation of the study includes a problem inherent to geometric morphometrics: the need for enough complete specimens. As major portions of hadrosauroid dentary morphology were to be mapped, these needed to be present in all specimens, which lowered the sample size to 84, and thus lowered potential statistical power. The limited sample size also meant that growth patterns had to be explored above the species level, indicating that some of the patterns we detected may be the result of interspecific, rather than intraspecific processes.

Finally, the following phylogenetic recommendations are made: (1) the use of characters pertaining to the anterior inclination of the coronoid process and the relative length of the edentulous region may be coded with non-hadrosaurid hadrosauroids of all ontogenetic stages, but saurolophids should only be coded for using adult specimens due to large ontogenetic variability in these regions; (2) the use of characters describing the shape and ventral deflection of the edentulous region and the amount of teeth per tooth row can be used to distinguish between non-hadrosaurid hadrosauroids and saurolophids, but only using adult specimens, as these regions are also ontogenetically variable in all taxonomic groups and further investigation concerning individual variability is merited as it is potentially high in the adults of some taxa; and (3) the addition of a ratio describing the relative height of the coronoid process to phylogenetic matrices is likely to provide a good distinction between non-hadrosaurid hadrosauroids and saurolophids.

**Acknowledgements.** This research was initially carried out as part of DFKS's MSc thesis at Uppsala University, examined by Professor Lars Holmer. We acknowledge the numerous collection managers and curators who provided specimen access to NEC and AP-M. Finally, we thank Taia Wyenberg-Henzler and Ali Nabavizadeh, whose reviews improved this manuscript. AB is supported by the postdoctoral grant ED481D-2021-026, funded by Xunta de Galicia, and by the 'Ramón y Cajal' fellowship (RYC2021-034269-I) of the MCIN/AEI/10.13039/501100011033 and the European Union <NextGenerationEU>/PRTR. AP-M was supported by the Ministry of Science and Innovation of the Government of Spain via the 'Ramón y Cajal' Program (RYC-2015-17388) and grant PID2020-119811GB-I00 funded by MCIN/AEI/10.13039/501100011033 and the CERCA Program funded by the Government of Catalonia. NEC is funded by an Australian Research Council Early Career Research Award (DE190101423). Open access publishing facilitated by University of New England, as part of the Wiley - University of New England agreement via the Council of Australian University Librarians.

**Author contributions.** **Conceptualization** DFK Söderblom (DFKS), NE Campione (NEC); **Data Curation** DFKS; **Formal Analysis** DFKS, NEC; **Investigation** DFKS; **Methodology** DFKS, NEC; **Project Administration** DFKS; **Resources** A Prieto-Márquez (AP-M), NEC. **Software** DFKS, NEC; **Supervision** DFKS, NEC; **Validation** DFKS, NEC; **Visualization** DFKS, A Blanco (AB), AP-M, NEC; **Writing – Original Draft Preparation** DFKS; **Writing – Review & Editing** DFKS, AB, AP-M, NEC.

## DATA ARCHIVING STATEMENT

Data for this study, including an R script, TPS file, and sliders file needed to run the analyses herein, intended to be used with a dataset (Appendix S1) are available in the Dryad Digital Repository: <https://doi.org/10.5061/dryad.p2ngf1vwm>

*Editor.* David Button

## SUPPORTING INFORMATION

Additional Supporting Information can be found online (<https://doi.org/10.1111/pala.12674>):

**Fig. S1.** Quantile–quantile (Q–Q) plots.

**Fig. S2.** Morphospace along principal components 3 and 4.

**Appendix S1.** Dataset for geometric morphometric analysis of hadrosauroid dentaries.

**Appendix S2.** Reference list for the hadrosauroid dentary dataset.

**Appendix S3.** Statistical summary of all 84 principal component axes.

**Appendix S4.** Detailed results from analysis of variance (ANOVA) and Tukey's honest significant difference test (TukeyHSD test).

**Appendix S5.** Detailed results from line-fitting (regression) analyses, and standardized major axis (SMA) estimation by genus and by clade/grade.

## REFERENCES

- ADAMS, D. C. and OTÁROLA-CASTILLO, E. 2013. Geomorph: an R package for the collection and analysis of geometric morphometric shape data. *Methods in Ecology & Evolution*, **4**, 393–399.
- ALBERCH, P., GOULD, S. J., OSTER, G. F. and WAKE, D. B. 1979. Size and shape in ontogeny and phylogeny. *Paleobiology*, **5**, 296–317.
- BELL, P. R. 2011. Cranial osteology and ontogeny of *Saurolophus angustirostris* from the Late Cretaceous of Mongolia with comments on *Saurolophus osborni* from Canada. *Acta Palaeontologica Polonica*, **56**, 703–722.
- BENSON, R. B. J., CAMPIONE, N. E., CARRANO, M. T., MANNION, P. D., SULLIVAN, C., UPCHURCH, P. and EVANS, D. C. 2014. Rates of dinosaur body mass evolution indicate 170 Million years of sustained ecological innovation on the avian stem lineage. *PLoS Biology*, **12**, e1001853.
- BENSON, R. B. J., HUNT, G., CARRANO, M. T. and CAMPIONE, N. 2018. Cope's rule and the adaptive landscape of dinosaur body size evolution. *Palaeontology*, **61**, 13–48.
- BLANCO, A., PRIETO-MÁRQUEZ, A. and DE ESTEBAN-TRIVIGNO, S. 2015. Diversity of hadrosauroid dinosaurs from the Late Cretaceous Ibero-Armorican Island (European Archipelago) assessed from dentary morphology. *Cretaceous Research*, **56**, 447–457.
- BOOKSTEIN, F. L., STREISSGUTH, A. P., SAMPSON, P. D., CONNOR, P. D. and BARR, H. M. 2002. Corpus callosum shape and neuropsychological deficits in adult males with heavy fetal alcohol exposure. *NeuroImage*, **15**, 233–251.
- BOULENGER, G. A. 1881. Sur l'arc pelvien chez les dinosauriens de Bernissart [On the pelvic arch in the dinosaurs of Bernissart]. *Bulletins de L'Académie royale de Belgique, 3eme Série*, **1**, 1–11.
- BRAMBLE, K., LEBLANC, A. R. H., LAMOUREUX, D. O., WOSIK, M. and CURRIE, P. J. 2017. Histological evidence for a dynamic dental battery in hadrosaurid dinosaurs. *Scientific Reports*, **7**, 1–13.
- BRINK, K. S., ZELENITSKY, D. K., EVANS, D. C., THERRIEN, F. and HORNER, J. R. 2011. A sub-adult skull of *Hypacrosaurus stebingeri* (Ornithischia: Lambeosaurinae): anatomy and comparison. *Historical Biology*, **23**, 63–72.
- BROWN, B. 1913. A new trachodont dinosaur, *Hypacrosaurus*, from the Edmonton Cretaceous of Alberta. *American Museum of Natural History Bulletin*, **32**, 395–406.
- CAMPIONE, N. E. and EVANS, D. C. 2011. Cranial growth and variation in edmontosaurs (Dinosauria: Hadrosauridae): implications for latest Cretaceous megaherbivore diversity in North America. *PLoS One*, **6**, e25186.
- CAMPIONE, N. E., BRINK, K. S., FREEDMAN, E. A., MCGARRITY, C. T. and EVANS, D. C. 2013. 'Glishades

- ericksoni*, an indeterminate juvenile hadrosaurid from the Two Medicine Formation of Montana: implications for hadrosaurid diversity in the latest Cretaceous (Campanian-Maastrichtian) of western North America. *Palaeobiodiversity & Palaeoenvironments*, **93**, 63–75.
- CARRANO, M. T., JANIS, C. M. and SEPKOSKI, J. J. Jr 1999. Hadrosaurs as ungulate parallels: lost lifestyles and deficient data. *Acta Palaeontologica Polonica*, **44**, 237–261.
- CASE, J. A., MARTIN, J. E., CHANEY, D. S., REGUERO, M., MARENSSI, S. A., SANTILLANA, S. M. and WOODBURNE, M. O. 2000. The first duck-billed dinosaur (Family Hadrosauridae) from Antarctica. *Journal of Vertebrate Paleontology*, **20**, 612–614.
- COLLYER, M. L. and ADAMS, D. C. 2013. Phenotypic trajectory analysis: comparison of shape change patterns in evolution and ecology. *Hystrix*, **24**, 75–83.
- COLLYER, M. L. and ADAMS, D. C. 2018. RRPP: an R package for fitting linear models to high-dimensional data using residual randomization. *Methods in Ecology & Evolution*, **9**, 1772–1779.
- COLLYER, M. L. and ADAMS, D. C. 2019. RRPP: linear model evaluation with randomized residuals in a permutation procedure. R package v1.3.1. <http://cran.r-project.org/package=RRPP>
- CRUZADO-CABALLERO, P. and CORIA, R. A. 2016. Revisiting the hadrosaurid (Dinosauria: Ornithopoda) diversity of the Allen Formation: a re-evaluation of *Willinakaqe salitralensis* from Salitral Moreno, Río Negro Province, Argentina. *Ameghiniana*, **53**, 231–237.
- CUTHBERTSON, R. S., TIRABASSO, A., RYBCZYNSKI, N. and HOLMES, R. B. 2012. Kinetic limitations of intracranial joints in *Brachylophosaurus canadensis* and *Edmontosaurus regalis* (Dinosauria: Hadrosauridae), and their implications for the chewing mechanics of hadrosaurids. *The Anatomical Record*, **295**, 968–979.
- ERICKSON, G. M., KRICK, B. A., HAMILTON, M., BOURNE, G. R., NORELL, M. A., LILLEODDEN, E. and SAWYER, W. G. 2012. Complex dental structure and wear biomechanics in hadrosaurid dinosaurs. *Science*, **338**, 98–101.
- EVANS, D. C. 2007. Ontogeny and evolution of lambeosaurine dinosaurs (Ornithischia: Hadrosauridae). PhD thesis, University of Toronto, Canada, 497pp.
- EVANS, D. C. 2010. Cranial anatomy and systematics of *Hypacrosaurus altispinus*, and a comparative analysis of skull growth in lambeosaurine hadrosaurids (Dinosauria: Ornithischia). *Zoological Journal of the Linnean Society*, **159**, 398–434.
- EVANS, D. C. and REISZ, R. R. 2007. Anatomy and relationships of *Lambeosaurus magnicristatus*, a crested hadrosaurid dinosaur (Ornithischia) from the Dinosaur Park Formation, Alberta. *Journal of Vertebrate Paleontology*, **27**, 373–393.
- FANTI, F., CAU, A., PANZARIN, L. and CANTELLI, L. 2016. Evidence of iguanodontian dinosaurs from the Lower Cretaceous of Tunisia. *Cretaceous Research*, **60**, 267–274.
- FARKE, A. A., CHOK, D. J., HERRERO, A., SCOLIERI, B. and WERNING, S. 2013. Ontogeny in the tube-crested dinosaur *Parasaurolophus* (Hadrosauridae) and heterochrony in hadrosaurids. *PeerJ*, **1**, e182.
- FRASER, D. and THEODOR, J. M. 2011. Comparing ungulate dietary proxies using discriminant function analysis. *Journal of Morphology*, **272**, 1513–1526.
- GANGLOFF, R. A. and FIORILLO, A. R. 2010. Taphonomy and paleoecology of a bonebed from the Prince Creek Formation, North Slope, Alaska. *PALAIOS*, **25**, 299–317.
- GATES, T. A., EVANS, D. C. and SERTICH, J. J. W. 2021. Description and rediagnosis of the crested hadrosaurid (Ornithopoda) dinosaur *Parasaurolophus cyrtocristatus* on the basis of new cranial remains. *PeerJ*, **9**, e10669.
- GODEFROIT, P., BOLOTSKY, Y. L. and VAN ITTERBEECK, J. 2004. The lambeosaurine dinosaur *Amurosaurus riabinini*, from the Maastrichtian of Far Eastern Russia. *Acta Palaeontologica Polonica*, **49**, 585–618.
- GODEFROIT, P., SHULIN, H., TINGXIANG, Y. and LAUTERS, P. 2008. New hadrosaurid dinosaurs from the uppermost Cretaceous of northeastern China. *Acta Palaeontologica Polonica*, **53**, 47–74.
- GUENTHER, M. F. 2009. Influence of sequence heterochrony on hadrosaurid dinosaur postcranial development. *The Anatomical Record*, **292**, 1427–1441.
- HEAD, J. J. 1998. A new species of basal hadrosaurid (Dinosauria, Ornithischia) from the Cenomanian of Texas. *Journal of Vertebrate Paleontology*, **18**, 718–738.
- HERRING, S. W., RAFFERTY, K. L., LIU, Z. J. and MARSHALL, C. D. 2001. Jaw muscles and the skull in mammals: the biomechanics of mastication. *Comparative Biochemistry & Physiology Part A: Molecular & Integrative Physiology*, **131**, 207–219.
- HILDEBRAND, G. Y. 1937. A further contribution to mandibular kinetics. *Journal of Dental Research*, **16**, 551–559.
- HORNER, J. R. and CURRIE, P. J. 1994. Embryonic and neonatal morphology and ontogeny of a new species of *Hypacrosaurus* (Ornithischia, Lambeosauridae) from Montana and Alberta. 312–336. In CARPENTER, K., HIRSCH, K. F. and HORNER, J. R. (eds) *Dinosaur eggs and babies*. Cambridge University Press.
- HORNER, J. R., WEISHAMPEL, D. B. and FORSTER, C. A. 2004. Hadrosauridae. 438–463. In WEISHAMPEL, D. B., DODSON, P. and OSMÓLSKA, H. (eds) *The Dinosauria*, Second edition. University of California Press, 861 pp.
- JANIS, C. M. and FORTELIUS, M. 1988. On the means whereby mammals achieve increased functional durability of their dentitions, with special reference to limiting factors. *Biological Reviews*, **63**, 197–230.
- KILIC, S., DIXON, P. M. and KEMPSON, S. A. 1997. A light microscopic and ultrastructural examination of calcified dental tissues of horses: 4. Cement and the amelocemental junction. *Equine Veterinary Journal*, **29**, 213–219.
- KIRKLAND, J. I. 1998. A new hadrosaurid from the Upper Cedar Mountain Formation (Albian-Cenomanian: Cretaceous) of eastern Utah - the oldest known hadrosaurid (lambeosaurine?). *Bulletin of the New Mexico Museum of Natural History & Science*, **14**, 283–295.
- KUBOTA, K. and KOBAYASHI, Y. 2009. Evolution of dentary diastema in iguanodontian dinosaurs. *Acta Geologica Sinica*, **83**, 39–45.

- LAMBE, L. M. 1917. A new genus and species of crestless hadrosaur from the Edmonton Formation of Alberta. *Ottawa Naturalist*, **31**, 65–73.
- LAMBE, L. M. 1920. The hadrosaur *Edmontosaurus* from the Upper Cretaceous of Alberta. *Geological Series*, **120**, 1–79.
- LEBLANC, A. R. H., REISZ, R. R., EVANS, D. C. and BAILLEUL, A. M. 2016. Ontogeny reveals function and evolution of the hadrosaurid dinosaur dental battery. *BMC Evolutionary Biology*, **16**, 152–164.
- LEHMAN, T. M., WICK, S. L. and WAGNER, J. R. 2016. Hadrosaurian dinosaurs from the Maastrichtian Javelina Formation, Big Bend National Park, Texas. *Journal of Paleontology*, **90**, 333–356.
- LEIDY, J. 1858. *Hadrosaurus foulkii*, a new saurian from the Cretaceous of New Jersey, related to *Iguanodon*. *Proceedings of the Academy of Natural Sciences of Philadelphia*, **10**, 213–218.
- LULL, R. S. and WRIGHT, N. E. 1942. Hadrosaurian dinosaurs of North America. *Geological Society of America Special Papers*, **40**, 1–242.
- MALLON, J. C. and ANDERSON, J. S. 2014. The functional and palaeoecological implications of tooth morphology and wear for the megaherbivorous dinosaurs from the Dinosaur Park Formation (Upper Campanian) of Alberta, Canada. *PLoS One*, **9**, e98605.
- MALLON, J. C. and ANDERSON, J. S. 2015. Jaw mechanics and evolutionary paleoecology of the megaherbivorous dinosaurs from the Dinosaur Park Formation (upper Campanian) of Alberta, Canada. *Journal of Vertebrate Paleontology*, **35**, e904323.
- MALLON, J. C., EVANS, D. C., RYAN, M. J. and ANDERSON, J. S. 2013. Feeding height stratification among the herbivorous dinosaurs from the Dinosaur Park Formation (upper Campanian) of Alberta, Canada. *BMC Ecology*, **13**, 1–15.
- MALLON, J. C., EVANS, D. C., ZHANG, Y. and XING, H. 2022. Rare juvenile material constrains estimation of skeletal allometry in *Gryposaurus notabilis* (Dinosauria: Hadrosauridae). *The Anatomical Record*, **306**, 25021.
- MARYAŃSKA, T. and OSMÓLSKA, H. 1981. Cranial anatomy of *Saurolophus angustirostris* with comments on the Asian Hadrosauridae (Dinosauria). *Palaeontologia Polonica*, **42**, 5–24.
- MCDONALD, A. T., WOLFE, D. G., FREEDMAN FOWLER, E. A. and GATES, T. A. 2021. A new brachylophosaurin (Dinosauria: Hadrosauridae) from the Upper Cretaceous Menefee Formation of New Mexico. *PeerJ*, **9**, e11084.
- MCGARRITY, C. T., CAMPIONE, N. E. and EVANS, D. C. 2013. Cranial anatomy and variation in *Prosaurolophus maximus* (Dinosauria: Hadrosauridae). *Zoological Journal of the Linnean Society*, **167**, 531–568.
- McNAMARA, K. J. 2012. Heterochrony: the evolution of development. *Evolution: Education & Outreach*, **5**, 203–218.
- MORI, H., DRUCKENMILLER, P. and ERICKSON, G. 2016. A new Arctic hadrosaurid (Dinosauria: Hadrosauridae) from the Prince Creek Formation (lower Maastrichtian) of northern Alaska. *Acta Palaeontologica Polonica*, **61**, 15–32.
- MOYANO, S. R., MORALES, M. M. and GIANNINI, N. P. 2020. Skull ontogeny of the pronghorn (*Antilocapra americana*) in the comparative context of native North American ungulates. *Canadian Journal of Zoology*, **98**, 165–174.
- NABAVIZADEH, A. 2014. Hadrosaurid jaw mechanics and the functional significance of the prementary bone. 467–482. In EBERTH, D. A. and EVANS, D. C. (eds) *Hadrosaurs*. Indiana University Press, 640 pp.
- NABAVIZADEH, A. 2016. Evolutionary trends in the jaw adductor mechanics of ornithischian dinosaurs: jaw mechanics in ornithischian dinosaurs. *The Anatomical Record*, **299**, 271–294.
- NABAVIZADEH, A. 2018. New reconstruction of cranial musculature in ornithischian dinosaurs: implications for feeding mechanisms and buccal anatomy. *The Anatomical Record*, **303**, 1–16.
- NABAVIZADEH, A. and WEISHAMPEL, D. B. 2016. The prementary bone and its significance in the evolution of feeding mechanisms in ornithischian dinosaurs. *The Anatomical Record*, **299**, 1358–1388.
- NORMAN, D. B. 1984. On the cranial morphology and evolution of ornithopod dinosaurs. *Symposium: Zoological Society of London*, **52**, 521–547.
- NORMAN, D. B. 1998. On Asian ornithopods (Dinosauria: Ornithischia). 3. A new species of iguanodontid dinosaur. *Zoological Journal of the Linnean Society*, **122**, 291–348.
- NORMAN, D. B. 2002. On Asian ornithopods (Dinosauria: Ornithischia). 4. *Probactrosaurus Rozhdestvensky*, 1966. *Zoological Journal of the Linnean Society*, **136**, 113–144.
- NORMAN, D. B. 2014. Iguanodonts from the Wealden of England: do they contribute to the discussion concerning hadrosaur origins? 10–43. In EBERTH, D. A. and EVANS, D. C. (eds) *Hadrosaurs*. Indiana University Press, 640 pp.
- NORMAN, D. B. and WEISHAMPEL, D. B. 1985. Ornithopod feeding mechanisms: their bearing on the evolution of herbivory. *The American Naturalist*, **126**, 151–164.
- ŐSI, A. and WEISHAMPEL, D. B. 2009. Jaw mechanism and dental function in the Late Cretaceous basal eusuchian *Iharkutosuchus*. *Journal of Morphology*, **270**, 903–920.
- ŐSI, A., BARRETT, P. M., FÖLDES, T. and TOKAI, R. 2014. Wear pattern, dental function, and jaw mechanism in the Late Cretaceous ankylosaur *Hungarosaurus*: jaw mechanism in *Hungarosaurus*. *The Anatomical Record*, **297**, 1165–1180.
- OSTROM, J. H. 1961. Cranial morphology of the hadrosaurian dinosaurs of North America. *Bulletin of the American Museum of Natural History*, **122**, 33–186.
- PARKS, W. A. 1922. *Parasaurolophus walkeri*, a new genus and species of crested trachodont dinosaur. *University of Toronto, Geological Series*, **15**, 5–57.
- PARKS, W. A. 1923. *Corythosaurus intermedius*, a new species of trachodont dinosaur. *University of Toronto, Geological Series*, **15**, 1–57.
- PRIETO-MÁRQUEZ, A. 2008. Phylogeny and historical biogeography of hadrosaurid dinosaurs. PhD thesis, University of Florida, USA, 861pp.
- PRIETO-MÁRQUEZ, A. 2010. Global phylogeny of Hadrosauridae (Dinosauria: Ornithopoda) using parsimony and Bayesian methods: phylogeny of hadrosaurid dinosaurs. *Zoological Journal of the Linnean Society*, **159**, 435–502.

- PRIETO-MÁRQUEZ, A. 2011. Cranial and appendicular ontogeny of *Bactrosaurus johnsoni*, a hadrosauroid dinosaur from the Late Cretaceous of northern China. *Palaeontology*, **54**, 773–792.
- PRIETO-MÁRQUEZ, A. 2014. A juvenile *Edmontosaurus* from the Late Maastrichtian (Cretaceous) of North America: implications for ontogeny and phylogenetic inference in saurolophine dinosaurs. *Cretaceous Research*, **50**, 282–303.
- PRIETO-MÁRQUEZ, A. and CARRERA FARIAS, M. Á. 2021. A new late-surviving early diverging Ibero-Armorican duck-billed dinosaur and the role of the Late Cretaceous European Archipelago in hadrosauroid biogeography. *Acta Palaeontologica Polonica*, **66**, 425–435.
- PRIETO-MÁRQUEZ, A. and GUTARRA, S. 2016. The ‘duck-billed’ dinosaurs of Careless Creek (Upper Cretaceous of Montana, USA), with comments on hadrosauroid ontogeny. *Journal of Paleontology*, **90**, 133–146.
- PRIETO-MÁRQUEZ, A., ERICKSON, G. M. and EBERSOLE, J. A. 2016. A primitive hadrosauroid from southeastern North America and the origin and early evolution of ‘duck-billed’ dinosaurs. *Journal of Vertebrate Paleontology*, **36**, e1054495.
- PRIETO-MÁRQUEZ, A., FONDEVILLA, V., SELLÉS, A. G., WAGNER, J. R. and GALOBART, A. 2019. *Adynomosaurus arcanus*, a new lambeosaurine dinosaur from the Late Cretaceous Ibero-Armorican Island of the European archipelago. *Cretaceous Research*, **96**, 19–37.
- POOLE, K. 2022. Placing juvenile specimens in phylogenies: an ontogenetically sensitive phylogenetic assessment of a new genus of iguanodontian dinosaur from the Early Cretaceous Kirkwood Formation, South Africa. *The Anatomical Record*, **306**, 25095.
- R CORE TEAM. 2013. R: a language and environment for statistical computing. R Foundation for Statistical Computing. <http://www.R-project.org>
- REILLY, S. M., McBRAYER, L. D. and WHITE, T. D. 2001. Prey processing in amniotes: biomechanical and behavioral patterns of food reduction. *Comparative Biochemistry & Physiology Part A: Molecular & Integrative Physiology*, **128**, 397–415.
- ROHLF, F. J. 2017a. tpsUtil. Department of Ecology & Evolution, State University of New York at Stony Brook. <https://www.sbmorphometrics.org/soft-utility.html>
- ROHLF, F. J. 2017b. tpsDIG2. Department of Ecology & Evolution, State University of New York at Stony Brook. <https://www.sbmorphometrics.org/soft-dataacq.html>
- RYBCZYNSKI, N., TIRABASSO, A., BLOSKIE, P., CUTHBERTSON, R. S. and HOLLIDAY, C. M. 2008. A three-dimensional animation model of *Edmontosaurus* (Hadrosauridae) for testing chewing hypotheses. *Palaeontologia Electronica*, **11**, 1–14.
- SCHOCH, R. R. 2014. Development and evolution. 152–190. In SCHOCH, R. R. *Amphibian evolution: The life of early land vertebrates*. Wiley Blackwell, 294 pp.
- SERENO, P. C. 1998. A rationale for phylogenetic definitions, with application to the higher-level taxonomy of Dinosauria. *Neues Jahrbuch für Geologie und Paläontologie, Abhandlungen*, **210**, 41–83.
- SHIBATA, M., JINTASAKUL, P., AZUMA, Y. and YOU, H.-L. 2015. A new basal hadrosauroid dinosaur from the Lower Cretaceous Khok Kruat Formation in Nakhon Ratchasima Province, northeastern Thailand. *PLoS One*, **10**, e0145904.
- SMITH, K. K. 2001. Heterochrony revisited: the evolution of developmental sequences. *Biological Journal of the Linnean Society*, **73**, 169–186.
- SÖDERBLOM, F., BLANCO, A., PRIETO-MÁRQUEZ, A. and CAMPIONE, N. 2023. Data from: The dentary of hadrosauroid dinosaurs: evolution through heterochrony. Dryad Digital Repository. <https://doi.org/10.5061/dryad.p2ngflvwm>
- SOLOUNIAS, N., DANOWITZ, M., BUTTAR, Z. and COOPEE, Z. 2019. Hypsodont crowns as additional roots: a new explanation for hypsodonty. *Frontiers in Ecology & Evolution*, **7**, 135.
- SPENCER, L. M. 1995. Morphological correlates of dietary resource partitioning in the African Bovidae. *Journal of Mammalogy*, **76**, 448–471.
- STUBBS, T. L., BENTON, M. J., ELSLER, A. and PRIETO-MÁRQUEZ, A. 2019. Morphological innovation and the evolution of hadrosauroid dinosaurs. *Paleobiology*, **45**, 347–362.
- TAKASAKI, R., FIORILLO, A. R., TYKOSKI, R. S. and KOBAYASHI, Y. 2020. Re-examination of the cranial osteology of the Arctic Alaskan hadrosaurine with implications for its taxonomic status. *PLoS One*, **15**, e0232410.
- TANOUE, K., GRANDSTAFF, B. S., YOU, H.-L. and DODSON, P. 2009. Jaw mechanics in basal Ceratopsia (Ornithischia, Dinosauria). *The Anatomical Record*, **292**, 1352–1369.
- TSOGTBAATAR, K., WEISHAMPEL, D. B., EVANS, D. C. and WATABE, M. 2014. A new hadrosauroid (*Plesiohadros djadokhtaensis*) from the Late Cretaceous Djadokhtan fauna of Southern Mongolia. 108–135. In EBERTH, D. A. and EVANS, D. C. (eds) *Hadrosaurs*. Indiana University Press, 640 pp.
- TSUIHIJI, T., WATABE, M., TSOGTBAATAR, K., TSUBAMOTO, T., BARSBOLD, R., SUZUKI, S., LEE, A. H., RIDGELY, R. C., KAWAHARA, Y. and WITMER, L. M. 2011. Cranial osteology of a juvenile specimen of *Tarbosaurus bataar* (Theropoda, Tyrannosauridae) from the Nemegt Formation (Upper Cretaceous) of Bugin Tsav, Mongolia. *Journal of Vertebrate Paleontology*, **31**, 497–517.
- TURNBULL, W. D. 1970. Mammalian masticatory apparatus. *Fieldiana*, **18**, 149–356.
- VARRIALE, F. J. 2016. Dental microwear reveals mammal-like chewing in the neoceratopsian dinosaur *Leptoceratops gracilis*. *PeerJ*, **4**, e2132.
- WARTON, D. I., DUURSMA, R. A., FALSTER, D. S. and TASKINEN, S. 2012. smatr 3- an R package for estimation and inference about allometric lines. *Methods in Ecology & Evolution*, **3**, 257–259.
- WEISHAMPEL, D. B. 1983. Hadrosauroid jaw mechanics. *Acta Palaeontologica Polonica*, **28**, 271–280.
- WEISHAMPEL, D. B. 1984. Evolution of jaw mechanisms in ornithomimid dinosaurs. *Advances in Anatomy, Embryology, & Cell Biology*, **87**, 1–109.
- WEISHAMPEL, D. B. and NORMAN, D. B. 1989. Vertebrate herbivory in the Mesozoic: jaws, plants, and evolutionary

- metrics. *Geological Society of America Special Paper*, **238**, 87–100.
- WEISHAMPEL, D. B., NORMAN, D. B. and GRIGORESCU, D. 1993. *Telmatosaurus transylvanicus* from the Late Cretaceous of Romania: the most basal hadrosaurid dinosaur. *Palaeontology*, **36**, 361–385.
- WOSIK, M., GOODWIN, M. B. and EVANS, D. C. 2019. Nestling-sized hadrosaurine cranial material from the Hell Creek Formation of northeastern Montana, USA, with an analysis of cranial ontogeny in *Edmontosaurus annectens*. *PaleoBios*, **36**, 1–18.
- WOSIK, M., CHIBA, K., THERRIEN, F. and EVANS, D. C. 2020. Testing size–frequency distributions as a method of ontogenetic aging: a life-history assessment of hadrosaurid dinosaurs from the Dinosaur Park Formation of Alberta, Canada, with implications for hadrosaurid paleoecology. *Paleobiology*, **46**, 379–404.
- WYENBERG-HENZLER, T. 2022. Ecomorphospace occupation of large herbivorous dinosaurs from Late Jurassic through to Late Cretaceous time in North America. *PeerJ*, **10**, e13174.
- WYENBERG-HENZLER, T., PATTERSON, R. T. and MALLON, J. C. 2022. Ontogenetic dietary shifts in North American hadrosaurids (Dinosauria: Ornithischia). *Cretaceous Research*, **135**, 105177.
- XING, H., WANG, D., HAN, F., SULLIVAN, C., MA, Q., HE, Y., HONE, D. W. E., YAN, R., DU, F. and XU, X. 2014. A new basal hadrosauroid dinosaur (Dinosauria: Ornithopoda) with transitional features from the Late Cretaceous of Henan Province, China. *PLoS One*, **9**, e98821.
- XING, H., MALLON, J. C. and CURRIE, M. L. 2017. Supplementary cranial description of the types of *Edmontosaurus regalis* (Ornithischia: Hadrosauridae), with comments on the phylogenetics and biogeography of Hadrosaurinae. *PLoS One*, **12**, e0175253.
- YOU, H., LUO, Z., SHUBIN, N. H., WITMER, L. M., TANG, Z. and TANG, F. 2003. The earliest-known duck-billed dinosaur from deposits of late Early Cretaceous age in northwest China and hadrosaur evolution. *Cretaceous Research*, **24**, 347–355.